

Exposure to electric or magnetic fields in the low and intermediate frequency range — Methods for calculating the current density and internal electric field induced in the human body —

Part 2-1: Exposure to magnetic fields — 2D models

The European Standard EN 62226-2-1:2005 has the status of a British Standard

ICS 17.220.20

National foreword

This British Standard is the official English language version of EN 62226-2-1:2005. It is identical with IEC 62226-2-1:2004.

The UK participation in its preparation was entrusted to Technical Committee GEL/106, Human exposure to Lf and Hf Electromagnetic radiation, which has the responsibility to:

- aid enquirers to understand the text;
- present to the responsible international/European committee any enquiries on the interpretation, or proposals for change, and keep the UK interests informed;
- monitor related international and European developments and promulgate them in the UK.

A list of organizations represented on this committee can be obtained on request to its secretary.

Cross-references

The British Standards which implement international or European publications referred to in this document may be found in the *BSI Catalogue* under the section entitled “International Standards Correspondence Index”, or by using the “Search” facility of the *BSI Electronic Catalogue* or of British Standards Online.

This publication does not purport to include all the necessary provisions of a contract. Users are responsible for its correct application.

Compliance with a British Standard does not of itself confer immunity from legal obligations.

Summary of pages

This document comprises a front cover, an inside front cover, the EN title page, pages 2 to 56, an inside back cover and a back cover.

The BSI copyright notice displayed in this document indicates when the document was last issued.

Amendments issued since publication

Amd. No.	Date	Comments

This British Standard was published under the authority of the Standards Policy and Strategy Committee on 11 February 2005

© BSI 11 February 2005

ISBN 0 580 45402 9

**Exposure to electric or magnetic fields
in the low and intermediate frequency range –
Methods for calculating the current density
and internal electric field induced in the human body
Part 2-1: Exposure to magnetic fields –
2D models
(IEC 62226-2-1:2004)**

Exposition aux champs électriques
ou magnétiques à basse
et moyenne fréquence –
Méthodes de calcul des densités
de courant induit et des champs
électriques induits dans le corps humain
Partie 2-1: Exposition à des champs
magnétiques –
Modèles 2D
(CEI 62226-2-1:2004)

Sicherheit in elektrischen oder
magnetischen Feldern im niedrigen und
mittleren Frequenzbereich –
Verfahren zur Berechnung der induzierten
Körperstromdichte und des im
menschlichen Körper induzierten
elektrischen Feldes
Teil 2-1: Exposition gegenüber
magnetischen Feldern –
2D-Modelle
(IEC 62226-2-1:2004)

This European Standard was approved by CENELEC on 2004-12-01. CENELEC members are bound to comply with the CEN/CENELEC Internal Regulations which stipulate the conditions for giving this European Standard the status of a national standard without any alteration.

Up-to-date lists and bibliographical references concerning such national standards may be obtained on application to the Central Secretariat or to any CENELEC member.

This European Standard exists in three official versions (English, French, German). A version in any other language made by translation under the responsibility of a CENELEC member into its own language and notified to the Central Secretariat has the same status as the official versions.

CENELEC members are the national electrotechnical committees of Austria, Belgium, Cyprus, Czech Republic, Denmark, Estonia, Finland, France, Germany, Greece, Hungary, Iceland, Ireland, Italy, Latvia, Lithuania, Luxembourg, Malta, Netherlands, Norway, Poland, Portugal, Slovakia, Slovenia, Spain, Sweden, Switzerland and United Kingdom.

CENELEC

European Committee for Electrotechnical Standardization
Comité Européen de Normalisation Electrotechnique
Europäisches Komitee für Elektrotechnische Normung

Central Secretariat: rue de Stassart 35, B - 1050 Brussels

Foreword

The text of document 106/79/FDIS, future edition 1 of IEC 62226-2-1, prepared by IEC TC 106, Methods for the assessment of electric, magnetic and electromagnetic fields associated with human exposure, was submitted to the IEC-CENELEC parallel vote and was approved by CENELEC as EN 62226-2-1 on 2004-12-01.

This Part 2-1 is to be used in conjunction with EN 62226-1¹⁾.

The following dates were fixed:

- latest date by which the EN has to be implemented at national level by publication of an identical national standard or by endorsement (dop) 2005-09-01
- latest date by which the national standards conflicting with the EN have to be withdrawn (dow) 2007-12-01

Endorsement notice

The text of the International Standard IEC 62226-2-1:2004 was approved by CENELEC as a European Standard without any modification.

1) To be published.

CONTENTS

INTRODUCTION.....	6
1 Scope	7
2 Analytical models	7
2.1 General.....	8
2.2 Basic analytical models for uniform fields	7
3 Numerical models.....	9
3.1 General information about numerical models.....	9
3.2 2D models – General approach.....	10
3.3 Conductivity of living tissues	11
3.4 2D Models – Computation conditions	12
3.5 Coupling factor for non-uniform magnetic field.....	12
3.6 2D Models – Computation results.....	13
4 Validation of models	15
Annex A (normative) Disk in a uniform field	16
Annex B (normative) Disk in a field created by an infinitely long wire.....	19
Annex C (normative) Disk in a field created by 2 parallel wires with balanced currents	27
Annex D (normative) Disk in a magnetic field created by a circular coil	38
Annex E (informative) Simplified approach of electromagnetic phenomena.....	50
Annex F (informative) Analytical calculation of magnetic field created by simple induction systems: 1 wire, 2 parallel wires with balanced currents and 1 circular coil.....	52
Annex G (informative) Equation and numerical modelling of electromagnetic phenomena for a typical structure: conductive disk in electromagnetic field.....	54
Bibliography	56
Figure 1 – Conducting disk in a uniform magnetic flux density.....	8
Figure 2 – Finite elements meshing (2 nd order triangles) of a disk, and detail	10
Figure 3 – Conducting disk in a non-uniform magnetic flux density.....	11
Figure 4 – Variation with distance to the source of the coupling factor for non-uniform magnetic field, K , for the three magnetic field sources (disk radius $R = 100$ mm).....	14
Figure A.1 – Current density lines J and distribution of J in the disk	16
Figure A.2 – $J = f[r]$: Spot distribution of induced current density calculated along a diameter of a homogeneous disk in a uniform magnetic field.....	17
Figure A.3 – $J_j = f[r]$: Distribution of integrated induced current density calculated along a diameter of a homogeneous disk in a uniform magnetic field.....	18
Figure B.1 – Disk in the magnetic field created by an infinitely straight wire	19
Figure B.2 – Current density lines J and distribution of J in the disk (<i>source: 1 wire, located at $d = 10$ mm from the edge of the disk</i>).....	20

Figure B.3 – Spot distribution of induced current density along the diameter AA of the disk (<i>source: 1 wire, located at $d = 10$ mm from the edge of the disk</i>)	20
Figure B.4 – Distribution of integrated induced current density along the diameter AA of the disk (<i>source: 1 wire, located at $d = 10$ mm from the edge of the disk</i>)	21
Figure B.5 – Current density lines J and distribution of J in the disk (<i>source: 1 wire, located at $d = 100$ mm from the edge of the disk</i>).....	21
Figure B.6 – Distribution of integrated induced current density along the diameter AA of the disk (<i>source: 1 wire, located at $d = 100$ mm from the edge of the disk</i>)	22
Figure B.7 – Parametric curve of factor K for distances up to 300 mm to a source consisting of an infinitely long wire (<i>disk: $R = 100$ mm</i>)	23
Figure B.8 – Parametric curve of factor K for distances up to 1 900 mm to a source consisting of an infinitely long wire (<i>disk: $R = 100$ mm</i>)	24
Figure B.9 – Parametric curve of factor K for distances up to 300 mm to a source consisting of an infinitely long wire (<i>disk: $R = 200$ mm</i>)	25
Figure B.10 – Parametric curve of factor K for distances up to 1 900 mm to a source consisting of an infinitely long wire (<i>disk: $R = 200$ mm</i>)	26
Figure C.1 – Conductive disk in the magnetic field generated by 2 parallel wires with balanced currents	27
Figure C.2 – Current density lines J and distribution of J in the disk (<i>source: 2 parallel wires with balanced currents, separated by 5 mm, located at $d = 7,5$ mm from the edge of the disk</i>).....	28
Figure C.3 – $J_i = f[r]$: Distribution of integrated induced current density calculated along the diameter AA of the disk (<i>source: 2 parallel wires with balanced currents, separated by 5 mm, located at $d = 7,5$ mm from the edge of the disk</i>)	28
Figure C.4– Current density lines J and distribution of J in the disk (<i>source: 2 parallel wires with balanced currents separated by 5 mm, located at $d = 97,5$ mm from the edge of the disk</i>).....	29
Figure C.5 – $J_i = f[r]$: Distribution of integrated induced current density calculated along the diameter AA of the disk (<i>source: 2 parallel wires with balanced currents separated by 5 mm, located at $d = 97,5$ mm from the edge of the disk</i>).....	29
Figure C.6 – Parametric curves of factor K for distances up to 300 mm to a source consisting of 2 parallel wires with balanced currents and for different distances e between the 2 wires (<i>homogeneous disk $R = 100$ mm</i>)	30
Figure C.7 – Parametric curves of factor K for distances up to 1 900 mm to a source consisting of 2 parallel wires with balanced currents and for different distances e between the 2 wires (<i>homogeneous disk $R = 100$ mm</i>)	32
Figure C.8 – Parametric curves of factor K for distances up to 300 mm to a source consisting of 2 parallel wires with balanced currents and for different distances e between the 2 wires (<i>homogeneous disk $R = 200$ mm</i>)	34
Figure C.9 – Parametric curves of factor K for distances up to 1 900 mm to a source consisting of 2 parallel wires with balanced currents and for different distances e between the 2 wires (<i>homogeneous disk $R = 200$ mm</i>)	36
Figure D.1 – Conductive disk in a magnetic field created by a coil.....	38
Figure D.2 –Current density lines J and distribution of J in the disk (<i>source: coil of radius $r = 50$ mm, conductive disk $R = 100$ mm, $d = 5$ mm</i>).....	39
Figure D.3 – $J_i = f[r]$: Distribution of integrated induced current density calculated along the diameter AA of the disk (<i>source: coil of radius $r = 50$ mm, conductive disk $R = 100$ mm, $d = 5$ mm</i>).....	39
Figure D.4 – Current density lines J and distribution of J in the disk (<i>source: coil of radius $r = 200$ mm, conductive disk $R = 100$ mm, $d = 5$ mm</i>).....	40

Figure D.5 – $J_i = f[r]$: Distribution of integrated induced current density calculated along the diameter AA of the disk (source: coil of radius $r = 200$ mm, conductive disk $R = 100$ mm, $d = 5$ mm)	40
Figure D.6 – Current density lines J and distribution of J in the disk (source: coil of radius $r = 10$ mm, conductive disk $R = 100$ mm, $d = 5$ mm)	41
Figure D.7 – $J_i = f[r]$: Distribution of integrated induced current density calculated along the diameter AA of the disk (source: coil of radius $r = 10$ mm, conductive disk $R = 100$ mm, $d = 5$ mm)	41
Figure D. 8 – Parametric curves of factor K for distances up to 300 mm to a source consisting of a coil and for different coil radius r (homogeneous disk $R = 100$ mm)	42
Figure D.9 – Parametric curves of factor K for distances up to 1 900 mm to a source consisting of a coil and for different coil radius r (homogeneous disk $R = 100$ mm)	44
Figure D.10 – Parametric curves of factor K for distances up to 300 mm to a source consisting of a coil and for different coil radius r (homogeneous disk $R = 200$ mm)	46
Figure D.11 – Parametric curves of factor K for distances up to 1 900 mm to a source consisting of a coil and for different coil radius r (homogeneous disk $R = 200$ mm)	48
Table 1 – Numerical values of the coupling factor for non-uniform magnetic field K for different types of magnetic field sources, and different distances between sources and conductive disk ($R = 100$ mm)	15
Table B.1 – Numerical values of factor K for distances up to 300 mm to a source consisting of an infinitely long wire (disk: $R = 100$ mm)	23
Table B.2 – Numerical values of factor K for distances up to 1 900 mm to a source consisting of an infinitely long wire (disk: $R = 100$ mm)	24
Table B.3 – Numerical values of factor K for distances up to 300 mm to a source consisting of an infinitely long wire (disk: $R = 200$ mm)	25
Table B.4 – Numerical values of factor K for distances up to 1 900 mm to a source consisting of an infinitely long wire (disk: $R = 200$ mm)	26
Table C.1 – Numerical values of factor K for distances up to 300 mm to a source consisting of 2 parallel wires with balanced currents (homogeneous disk: $R = 100$ mm)	31
Table C.2 – Numerical values of factor K for distances up to 1 900 mm to a source consisting of 2 parallel wires with balanced currents (homogeneous disk: $R = 100$ mm)	33
Table C.3 – Numerical values of factor K for distances up to 300 mm to a source consisting of 2 parallel wires with balanced currents (homogeneous disk: $R = 200$ mm)	35
Table C.4 – Numerical values of factor K for distances up to 1 900 mm to a source consisting of 2 parallel wires with balanced currents (homogeneous disk: $R = 200$ mm)	37
Table D.1 – Numerical values of factor K for distances up to 300 mm to a source consisting of a coil (homogeneous disk: $R = 100$ mm)	43
Table D.2 – Numerical values of factor K for distances up to 1 900 mm to a source consisting of a coil (homogeneous disk: $R = 100$ mm)	45
Table D.3 – Numerical values of factor K for distances up to 300 mm to a source consisting of a coil (homogeneous disk: $R = 200$ mm)	47
Table D.4 – Numerical values of factor K for distances up to 1 900 mm to a source consisting of a coil (homogeneous disk: $R = 200$ mm)	49

INTRODUCTION

Public interest concerning human exposure to electric and magnetic fields has led international and national organisations to propose limits based on recognised adverse effects.

This standard applies to the frequency range for which the exposure limits are based on the induction of voltages or currents in the human body, when exposed to electric and magnetic fields. This frequency range covers the low and intermediate frequencies, up to 100 kHz. Some methods described in this standard can be used at higher frequencies under specific conditions.

The exposure limits based on biological and medical experimentation about these fundamental induction phenomena are usually called “basic restrictions”. They include safety factors.

The induced electrical quantities are not directly measurable, so simplified derived limits are also proposed. These limits, called “reference levels”, are given in terms of external electric and magnetic fields. They are based on very simple models of coupling between external fields and the body. These derived limits are conservative.

Sophisticated models for calculating induced currents in the body have been used and are the subject of a number of scientific publications. These use numerical 3D electromagnetic field computation codes and detailed models of the internal structure with specific electrical characteristics of each tissue within the body. However such models are still developing; the electrical conductivity data available at present has considerable shortcomings; and the spatial resolution of models is still advancing. Such models are therefore still considered to be in the field of scientific research and at present it is not considered that the results obtained from such models should be fixed indefinitely within standards. However it is recognised that such models can and do make a useful contribution to the standardisation process, specially for product standards where particular cases of exposure are considered. When results from such models are used in standards, the results should be reviewed from time to time to ensure they continue to reflect the current status of the science.

**EXPOSURE TO ELECTRIC OR MAGNETIC FIELDS
IN THE LOW AND INTERMEDIATE FREQUENCY RANGE –
METHODS FOR CALCULATING THE CURRENT DENSITY
AND INTERNAL ELECTRIC FIELD INDUCED IN THE HUMAN BODY –**

**Part 2-1: Exposure to magnetic fields –
2D models**

1 Scope

This part of IEC 62226 introduces the coupling factor K , to enable exposure assessment for complex exposure situations, such as non-uniform magnetic field or perturbed electric field. The coupling factor K has different physical interpretations depending on whether it relates to electric or magnetic field exposure.

The aim of this part is to define in more detail this coupling factor K , for the case of simple models of the human body, exposed to non-uniform magnetic fields. It is thus called “coupling factor for non-uniform magnetic field”.

All the calculations developed in this document use the low frequency approximation in which displacement currents are neglected. This approximation has been validated in the low frequency range in the human body where parameter $\varepsilon\omega \ll \sigma$.

For frequencies up to a few kHz, the ratio of conductivity and permittivity should be calculated to validate this hypothesis.

2 Analytical models

2.1 General

Basic restrictions in guidelines on human exposure to magnetic fields up to about 100 kHz are generally expressed in terms of induced current density or internal electric field. These electrical quantities cannot be measured directly and the purpose of this document is to give methods and tools on how to assess these quantities from the external magnetic field.

The induced current density J and the internal electric field E_i are closely linked by the simple relation:

$$J = \sigma E_i \quad (1)$$

where σ is the conductivity of living tissues.

For simplicity, the content of this standard is presented in terms of induced current densities J , from which values of the internal electric field can be easily derived using the previous formula.

Analytical models have been used in EMF health guidelines to quantify the relationship between induced currents or internal electric field and the external fields. These involve assumptions of highly simplified body geometry, with homogeneous conductivity and uniform applied magnetic field. Such models have serious limitations. The human body is a much more complicated non-homogeneous structure, and the applied field is generally non-uniform because it arises from currents flowing through complex sets of conductors and coils.

For example, in an induction heating system, the magnetic field is in fact the superposition of an excitation field (created by the coils), and a reaction field (created by the induced currents in the piece). In the body, this reaction field is negligible and can be ignored.

Annex E and F presents the analytical calculation of magnetic field H created by simple sources and Annex G presents the analytical method for calculating the induced current in a conductive disk.

2.2 Basic analytical models for uniform fields

The simplest analytical models used in EMF health guidelines are based on the hypothesis of coupling between a uniform external magnetic field at a single frequency, and a homogeneous disk of given conductivity, used to represent the part of the body under consideration, as illustrated in Figure 1. Such models are used for example in the ICNIRP ¹⁾ and NRPB ²⁾ guidelines.

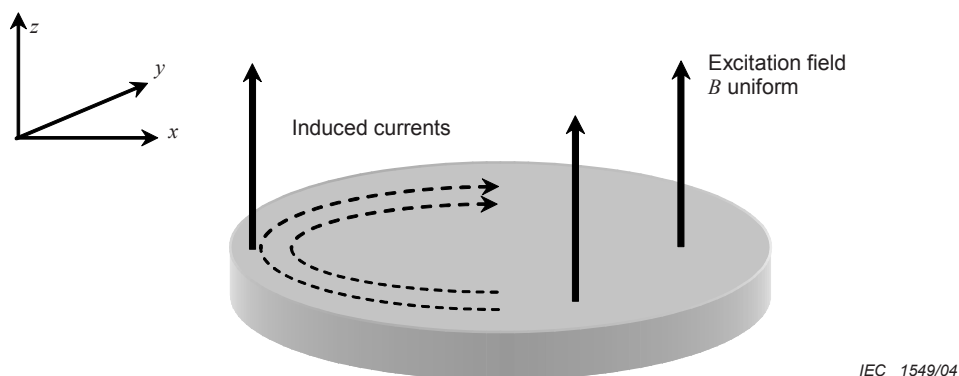


Figure 1 – Conducting disk in a uniform magnetic flux density

The objective of such a modelling is to provide a simple method to assess induced currents and internal fields. This very first approach is simple and gives conservative values of the electrical quantities calculated.

For alternating magnetic fields, the calculation assumes that the body or the part of the body exposed is a circular section of radius r , with conductivity σ . The calculation is made under maximum coupling conditions i.e. with a uniform magnetic field perpendicular to this disk. In this case, the induced current density at radius r is given by:

$$J(r) = \frac{r\sigma}{2} \frac{dB}{dt} \quad (2)$$

where B is the magnetic flux density.

1) Health Physics (vol. 74, n° 4, April 1998, pp 496-522).

2) NRPB, 1993, Board Statement on Restrictions on Human Exposure to Static and Time-varying Electromagnetic Fields and Radiation, Volume 4, No 5, 1.

For a single frequency f , this becomes:

$$J(r) = \sigma \pi r f B \quad (3)$$

As illustrated in Figure 1 (see also Annex A), induced currents are distributed inside the disk, following a rotation symmetry around the central axis of the disk. The value of induced currents is minimum (zero) at the centre and maximum at the edge of the disk.

3 Numerical models

3.1 General information about numerical models

Simple models, which take into consideration field characteristics, are more realistic than those, which consider only uniform fields, such as analytical ones.

Electromagnetic fields are governed by Maxwell's equations. These equations can be accurately solved in 2- or 3-dimensional structures (2D or 3D computations) using various numerical methods, such as:

- finite elements method (FEM);
- boundary integral equations method (BIE or BEM), or moment method;
- finite differences method (FD);
- impedance method (IM).

Others methods derive from these. For example, the following derive from the finite differences method:

- finite difference time domain (FDTD);
- frequency dependent finite difference time domain ((FD)²TD);
- scalar potential finite difference (SPFD).

Hybrid methods have been also developed in order to improve modelling (example: FE + BIE).

Commercially available software can accurately solve Maxwell's equations by taking into account real geometrical structures and physical characteristics of materials, as well as in steady state or transient current source conditions.

The choice of the numerical method is guided by a compromise between accuracy, computational efficiency, memory requirements, and depends on many parameters, such as:

- simulated field exposure;
- size and shape of human object to be modelled;
- description level of the human object (size of voxel), or fineness of the meshing;
- frequency range, in order to neglect some parts of Maxwell's relations (example: displacement current term for low frequency);
- electrical supply signal (sinusoidal, periodic or transient);

- type of resolution (2D or 3D);
- mathematical formulation;
- linear or non linear physical parameters (conductivity, ...);
- performances of the numerical method;
- etc.

Computation times can therefore vary significantly.

Computed electromagnetic values can be presented in different ways, including:

- distributions of magnetic field H , flux density B , electric field E , current density J . These distributions can be presented in the form of coloured iso-value lines and/or curves, allowing a visual assessment of the phenomena and the possible "hot" points;
- local or spatial averaged integral values of H , B , E , J , etc.;
- global magnitude values: active power.

These methods are very helpful for solving specific problems; however they cannot be conveniently used to study general problems.

3.2 2D models – General approach

In order to gain quickly an understanding of induced currents in the human body, 2D simulations can be performed using a simple representation of the body (a conductive disk: example of modelling given in Figure 2) in a non-uniform magnetic field, as illustrated in Figure 3.

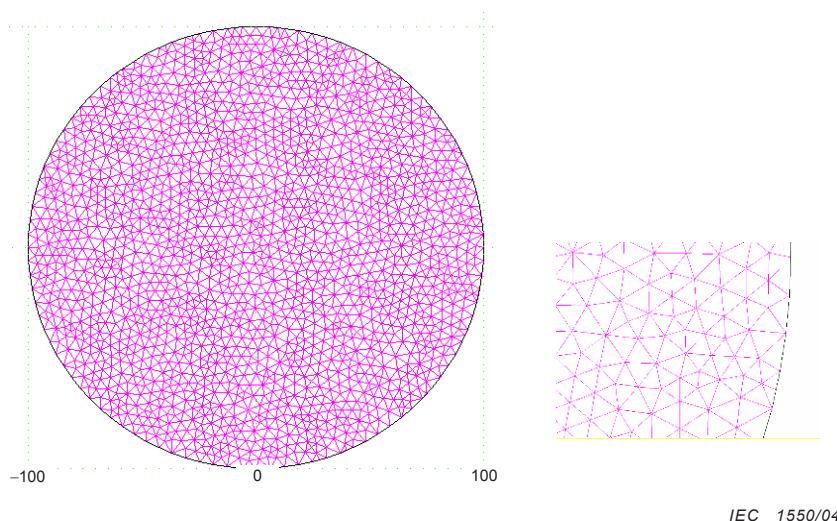


Figure 2 – Finite elements meshing (2nd order triangles) of a disk, and detail

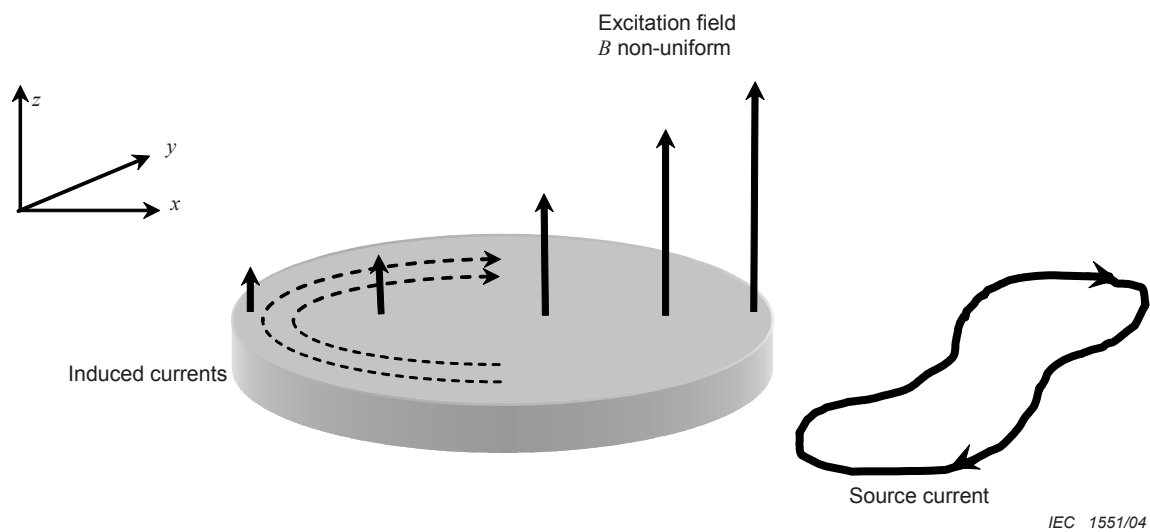


Figure 3 – Conducting disk in a non-uniform magnetic flux density

Starting from Maxwell's relations (low frequency approximation), a single equation can be obtained with a specific mathematical formulation (see Annex G):

$$\frac{1}{\sigma} \nabla^2 \vec{H}_r - \mu_0 \frac{\partial \vec{H}_r}{\partial t} = \mu_0 \frac{\partial \vec{H}_{ex}}{\partial t} \quad (4)$$

where

H_{ex} is the excitation field created by the source currents,

H_r is the reaction field created by the induced currents:

$$\vec{J} = \text{Curl}(\vec{H}_r) \quad (5)$$

Equation (4) is solved for a 2D geometry using the finite element method applied to the meshing illustrated in Figure 2.

The excitation field H_{ex} is calculated for three non-uniform field sources using the analytical expressions given in Annex F. The three sources modelled are: a current flowing through an infinitely long wire, two parallel wires with balanced currents and a current loop.

X, Y, Z co-ordinates are used. XY -plane is the study plane of the disk in which induced currents are generated. Except for the particular case where H_{ex} is uniform, source currents are in the same plane. Only the one component of H_{ex} along the Z -axis is taken into account. The induced currents in the disk have two components J_x, J_y .

Examples of numerical results are presented in Annexes A to D.

3.3 Conductivity of living tissues

The computation of induced currents in the body from the external magnetic field is strongly affected by the conductivity of the different tissues in the body and their anisotropic properties. The results presented in this document assume that the conductivity is homogeneous and isotropic with a value of 0,2 S/m. This value is consistent with the average value assumed in EMF health guidelines.

The most recent assessment of the available data indicates the average conductivity to be slightly higher: 0,22 S/m. More experimental work is in progress to provide more reliable conductivity information. The preferred average conductivity could be changed in the future as improved information becomes available. In that situation the values of induced current presented in this report should be revised in proportion to the conductivity. Nevertheless, the coupling factor for non-uniform magnetic field K , defined previously, is independent of the conductivity.

3.4 2D Models – Computation conditions

2D computation codes were used to simulate the current induced in a conductive disk by an alternating magnetic field of frequency f , produced by four different field sources:

- uniform and unidirectional field in all considered space (Annex A);
- current flowing through one infinitely long wire (Annex B);
- 2 parallel wires with balanced currents (Annex C);
- current flowing through one circular coil. (Annex D).

In order to facilitate comparisons with analytical models, all numerical values of computation parameters are fixed throughout this standard:

- radius of disk: $R = 100$ mm, and $R = 200$ mm;
- conductivity of disk: $\sigma = 0,2$ S/m;
- field sources at 50 Hz frequency.

With the exception of the first of the four field sources, the magnetic field from the source is non-uniform, decreasing with increasing distance from the source. In these cases the field value quoted is the value at the edge of the disk closest to the source.

The reaction field created by the induced current in the disk is negligible (due to the very low conductivity of the disk) and is ignored.

3.5 Coupling factor for non-uniform magnetic field

The current density induced in the disk by a localised source of magnetic field (therefore generating a non-uniform field), is always lower than the current density that would be induced by a uniform magnetic field whose magnitude is equal to the magnitude of the non-uniform field at the edge of the disk closest to the localised source. This reduction of induced current for non-uniform field sources is quantified using the coupling factor for non-uniform magnetic field K , which is physically defined as:

$$K = \frac{J_{\text{nonuniform}}}{J_{\text{uniform}}} \quad (6)$$

where

$J_{\text{nonuniform}}$ is the maximum induced current density in the disk exposed to the non-uniform magnetic field from a localised source,

J_{uniform} is the maximum induced current density in the disk exposed to a uniform magnetic field.

J_{uniform} is derived from equation (3):

$$J_{\text{uniform}} = J(r = R) = \sigma \pi R f B \quad (7)$$

It shall be noted that $K = 1$ when the field is uniform. Annex A illustrates the current distribution in a disk of radius $R = 100$ mm for an applied uniform field $B = 1,25$ μ T. The coupling factor for non-uniform magnetic field K is calculated numerically for the three non-uniform sources of field, in Annex B, C and D respectively.

NOTE 1 Calculated spot values of induced current densities have been averaged in this document (see Annexes A to D). So the values of J_{uniform} and $J_{\text{nonuniform}}$ given here above are averaged values, integrated over a cross section of 1 cm^2 , perpendicular to the current direction.

NOTE 2 Values of K are calculated at a frequency of 50 Hz. Nevertheless, due to the low frequency approximation, these values are also valid for the whole frequency range covered by this standard i.e. up to 100 kHz. Also, due to the low frequency approximation, K is independent of the conductivity.

For real cases, the spatial arrangement of field cannot easily be described in equations, and the coupling factor K can only be estimated (for example using the table values given in annexes of this document).

3.6 2D Models – Computation results

This subclause is a summary of the detailed numerical results given in Annexes B, C and D, which deal with the three types of sources. Whatever the source, the model of human body is treated as a homogeneous disk:

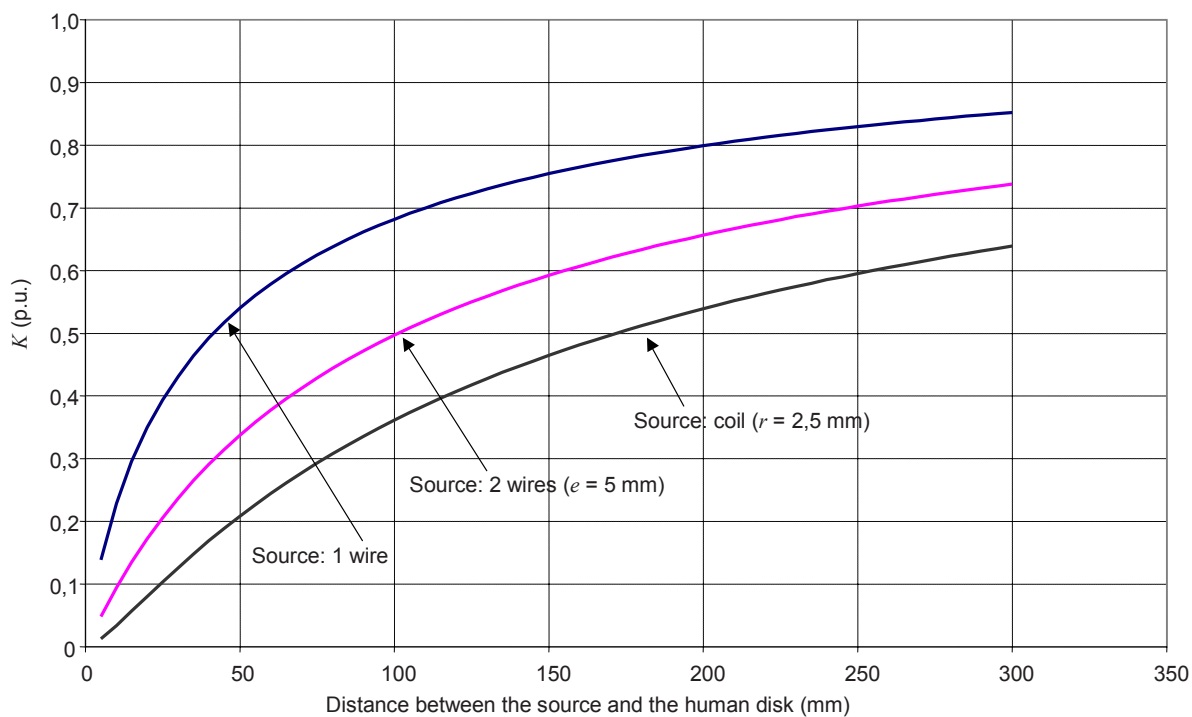
- radius of disk: $R = 100$ mm and $R = 200$ mm;
- conductivity of disk: $\sigma = 0,2$ S/m .

For comparison between the different types of sources (i.e. coupling models), the value of the local maximum magnetic field is normalised. Whatever the source, the magnetic field magnitude at the edge of the disk closest to the source is equal to the uniform field magnitude (i.e. $B = 1,25$ μ T, see annex A).

Table 1 presents a selection from Annexes B, C and D of the numerical values of the factor K for the three different sources and for a disk radius $R = 100$ mm. These results are also presented in a graphic form in Figure 4.

All the values in Table 1 are less than 1, and sometimes much less than 1, by a factor up to about 100. This demonstrates that, for a specified maximum current density in the disk, the corresponding magnetic field at the edge of the disk can have a wide range of values depending on the characteristics of the field source and on the distance between the disk and source.

The uniform field approximation (for which $K = 1$) is appropriate only when the distance between the source and the “human disk” becomes large relative to the size of the disk (typically 10 times the disk radius). At more usual distance of exposure from, for example, domestic appliances, the non-uniformity of the magnetic field with the distance has to be taken into account in the way presented in this standard.



IEC 1552/04

NOTE Values for distances up to 1 900 mm, and for other wire separations and coil sizes are given in Annexes B, C and D.

Figure 4 – Variation with distance to the source of the coupling factor for non-uniform magnetic field, K , for the three magnetic field sources (disk radius $R = 100$ mm)

Table 1 – Numerical values of the coupling factor for non-uniform magnetic field K for different types of magnetic field sources, and different distances between sources and conductive disk ($R = 100$ mm)

K factor for different sources			
Distance between the source and the disk mm	1 infinite wire	2 parallel wires with balanced currents, 5 mm spaced	1 circular coil 2,5 mm radius
10	0,229	0,094	0,034
20	0,350	0,172	0,080
30	0,432	0,237	0,126
40	0,492	0,291	0,169
50	0,540	0,337	0,208
60	0,579	0,378	0,244
70	0,611	0,413	0,277
80	0,638	0,444	0,308
90	0,661	0,472	0,336
100	0,682	0,497	0,361
110	0,700	0,520	0,385
120	0,716	0,540	0,407
130	0,730	0,559	0,428
140	0,743	0,576	0,447
150	0,754	0,592	0,465
160	0,765	0,607	0,482
170	0,775	0,621	0,497
180	0,783	0,634	0,512
190	0,792	0,645	0,526
200	0,799	0,657	0,539
210	0,806	0,667	0,552
220	0,813	0,677	0,563
230	0,819	0,686	0,575
240	0,824	0,695	0,585
250	0,830	0,703	0,595
260	0,835	0,711	0,605
270	0,839	0,718	0,614
280	0,844	0,725	0,623
290	0,848	0,732	0,631
300	0,852	0,738	0,639

NOTE Values for distances up to 1 900 mm, and for other wire separations and coil sizes are given in Annexes B, C and D.

4 Validation of models

The validation of the numerical tools used for computation of induced current densities shall be made by comparison with the results given in the annexes of this standard, which have been validated by comparison with scientific literature.

Additional information concerning the software used for the validation of numerical computation can be found in the bibliographic references of IEC 62226-1.

Annex A (normative)

Disk in a uniform field

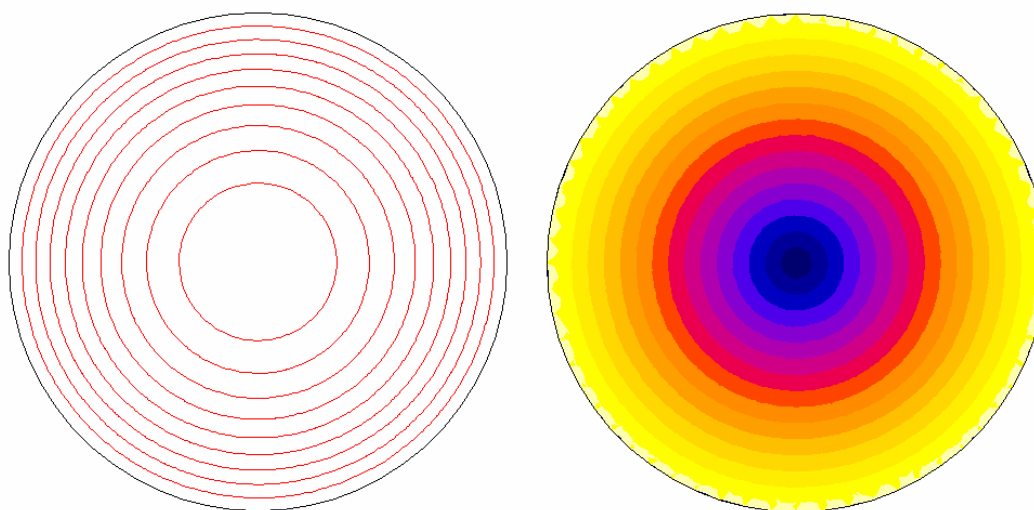
The induced currents are calculated in a disk of homogeneous conductivity. In order to allow comparison between different field sources configurations (depending on geometry of the source and distance to the disk, see Annex B to D) the following standard values have been chosen:

- f , frequency = 50 Hz (see note 2 in 3.5);
- B , uniform magnetic flux density = 1,25 μT ;
- R , radius of the conductive disk = 100 mm;
- σ , conductivity (homogeneous) = 0,2 S/m.

Using these values in equation (3) gives, at the edge of the disk:

$$J_{\max} = 0,393 \times 10^{-5} \text{ A/m}^2 \text{ (analytical calculation)}$$

Results of a numerical computation using finite element methods are presented hereafter in the form of graphs giving the shape of the distribution of induced currents in the disk (Figure A.1) and curve giving numerical values of local induced currents (Figure A.2):



IEC 1553/04

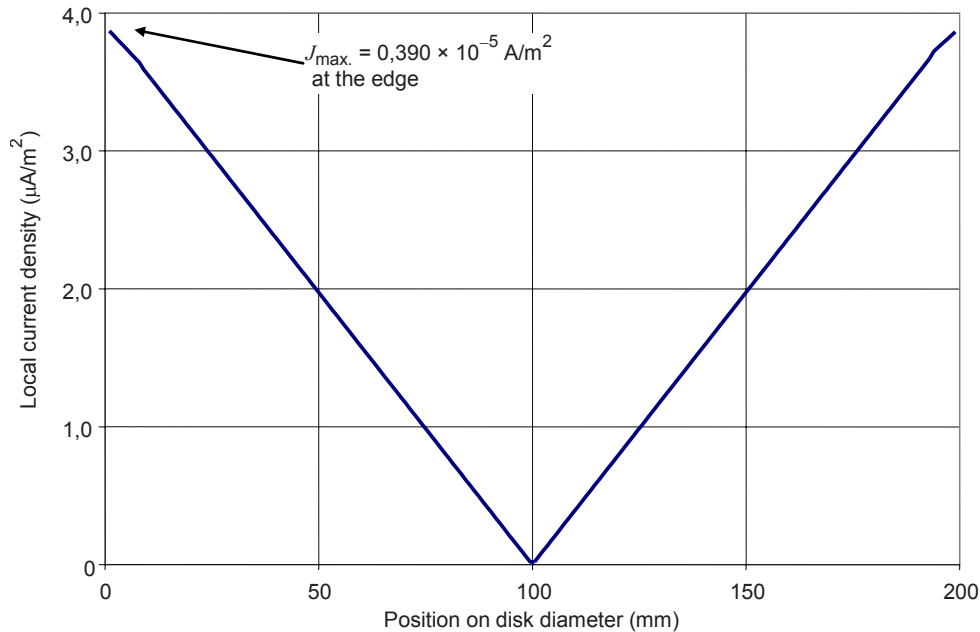
Figure A.1 – Current density lines J and distribution of J in the disk

This computation gives, at the edge of the disk a value of:

$$J_{\max} = 0,390 \times 10^{-5} \text{ A/m}^2$$

Considering the meshing effect of numerical models, this numerical value of J_{\max} can be considered as equal to the analytical one. So, analytical and numerical approaches give very similar results in this simple case.

The induced current density varies linearly with distance along a diameter of the disk as shown in Figure A.2:



IEC 1554/04

Figure A.2 – $J = f[r]$: Spot distribution of induced current density calculated along a diameter of a homogeneous disk in a uniform magnetic field

To avoid any bias due to numerical meshing, calculated spot values shall be averaged. In the computations of the present document, a square section of 1 cm², perpendicular to the current direction was used.

The corresponding analytical formula is the integral of equation (3):

$$J_i(r) = 1/r_m \int_{r-r_m/2}^{r+r_m/2} \sigma \pi f \alpha B d\alpha \quad (\text{A-1})$$

where r_m is the length of integration, equal to 1 cm (valid for $r < R - r_m/2$)

Using the numerical values previously defined, the analytical solution of equation (A-1) is:

$$J_{i \max} = 0,375 \times 10^{-5} \text{ A/m}^2$$

which is very similar to the numerical value: $J_{i \max} = 0,374 \times 10^{-5} \text{ A/m}^2$.

Due to the integration, this value is lower than the spot value.

The distribution of the integrated induced current density is also a linear function of the position of calculation point along a diameter of the disk, as illustrated in Figure A.3:

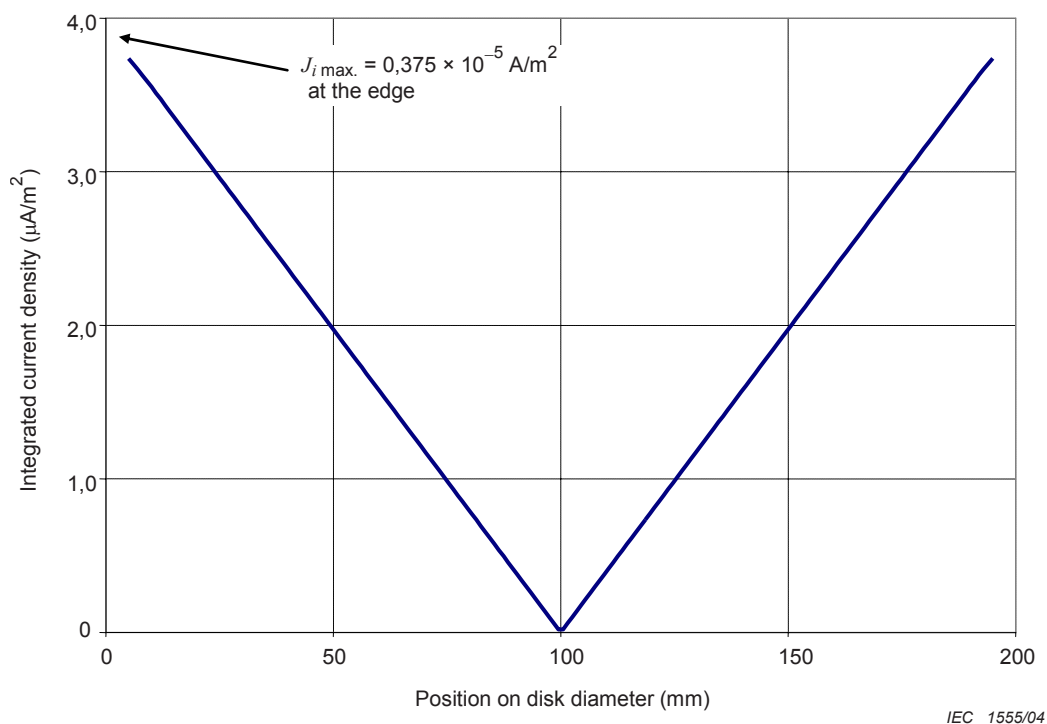


Figure A.3 – $J_i = f[r]$: Distribution of integrated induced current density calculated along a diameter of a homogeneous disk in a uniform magnetic field

Annex B (normative)

Disk in a field created by an infinitely long wire

The induced currents are calculated in a disk of homogeneous conductivity. In order to allow comparison between different field sources configurations (depending on geometry of the source and distance to the disk) the following standard values have been chosen:

- f , frequency = 50 Hz (see note 2 of 3.5);
- B , magnetic flux density = 1,25 μT , at the edge of the disk closer to the field source;
- R , radius of the conductive disk = 100 mm or 200 mm;
- σ , conductivity (homogeneous) = 0,2 S/m.

In this annex, the field source is an alternating current flowing through an infinite straight wire. The conductive disk and the field source are located in the same plane, at a distance d (see Figure B.1).

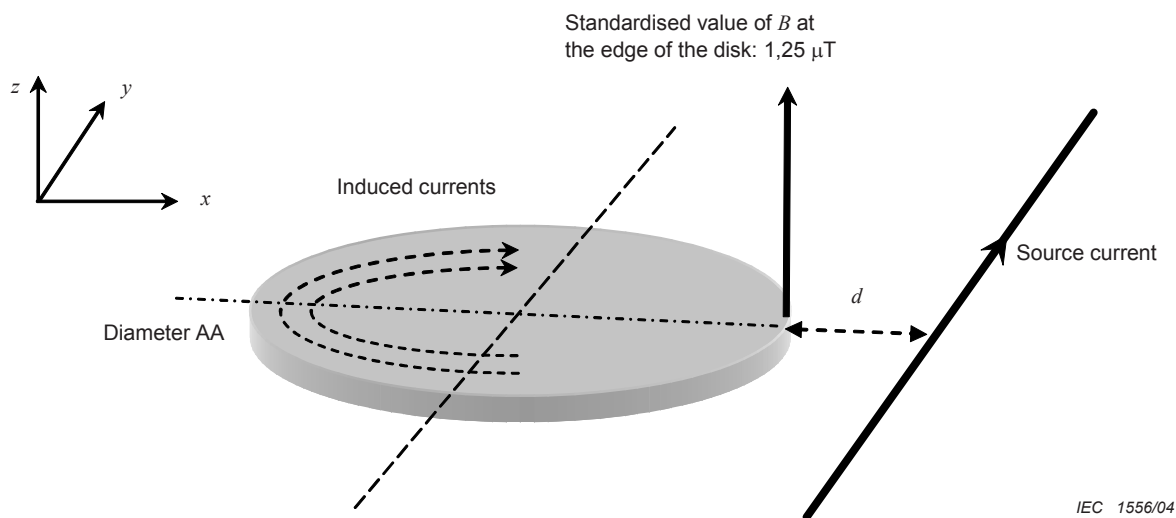


Figure B.1 – Disk in the magnetic field created by an infinitely straight wire

The distance d is the minimum distance between the edge of the disk and the closer part of the source.

The variation of the coupling factor for non-uniform magnetic field K is studied with regard to the distance d for:

- exposure close to the source: $0 < d < 300$ mm
- exposure at higher distance: $0 < d < 1\,900$ mm

For illustrations and examples of induced currents computation, 3 distances d have been studied:

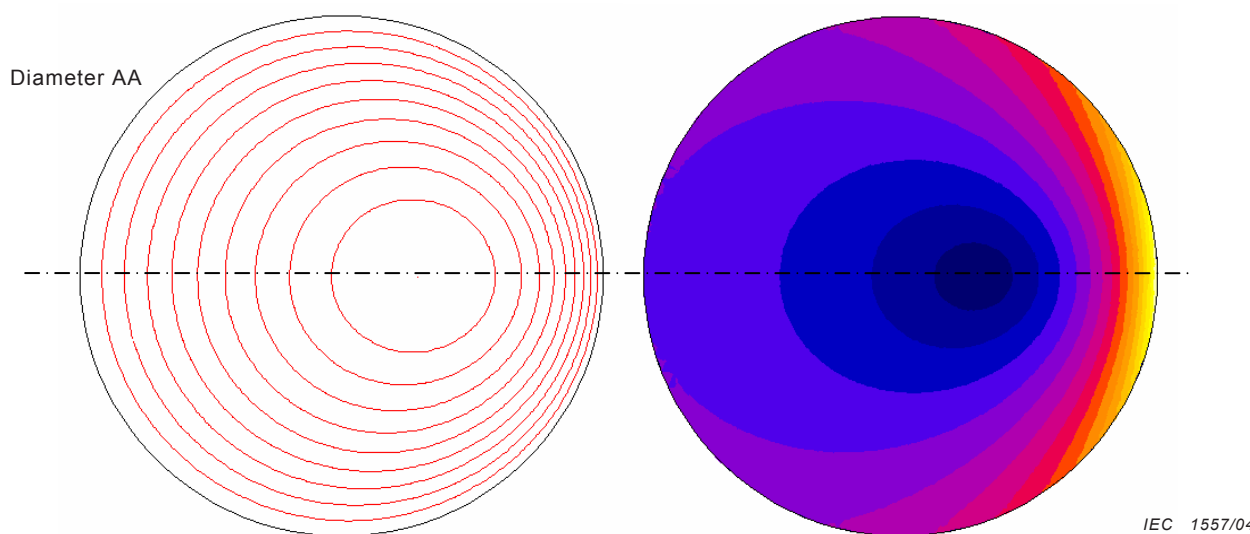
- $d = 10$ mm;
- $d = 100$ mm;
- $d = 1\,000$ mm.

B.1 Calculations for a conductive disk with a radius $R = 100$ mm

B.1.1 Examples of calculation of induced currents in the disk

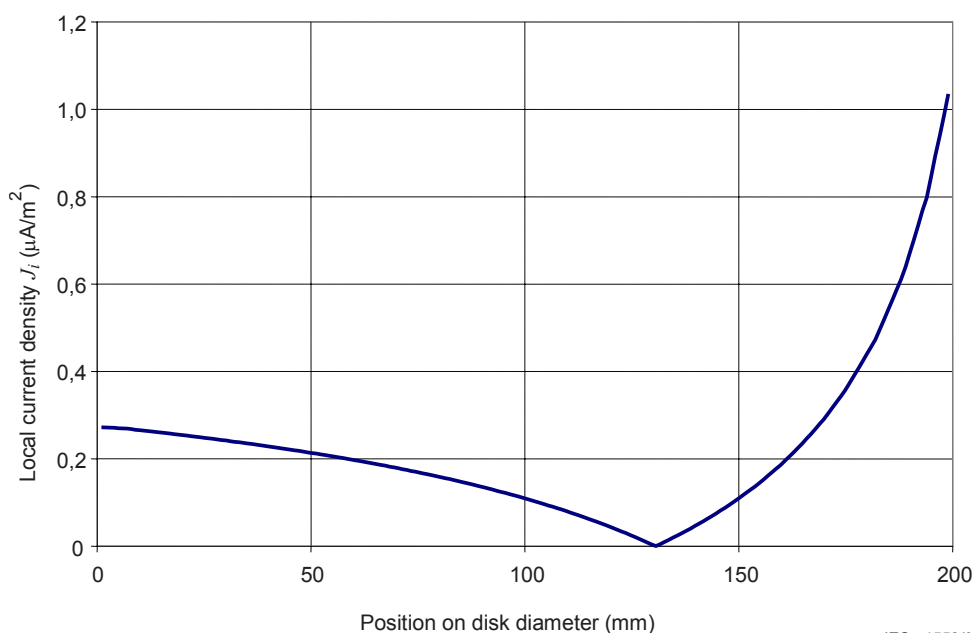
B.1.1.1 Distance to the source $d = 10$ mm

Results of the computation of local induced currents in the disk are given hereunder in form of graphs giving the shape of the distribution of induced currents in the disk (Figure B.2) and curves giving numerical values of the induced currents (Figures B.3 and B.4). The curve in Figure B.4 gives the distribution of the induced currents integrated over a surface of 1 cm^2 perpendicular to the induced current direction.



IEC 1557/04

Figure B.2 – Current density lines J and distribution of J in the disk (source: 1 wire, located at $d = 10$ mm from the edge of the disk)



IEC 1558/04

Figure B.3 – Spot distribution of induced current density along the diameter AA of the disk (source: 1 wire, located at $d = 10$ mm from the edge of the disk)

NOTE The diameter AA is located as illustrated in Figures B.1 and B.2.

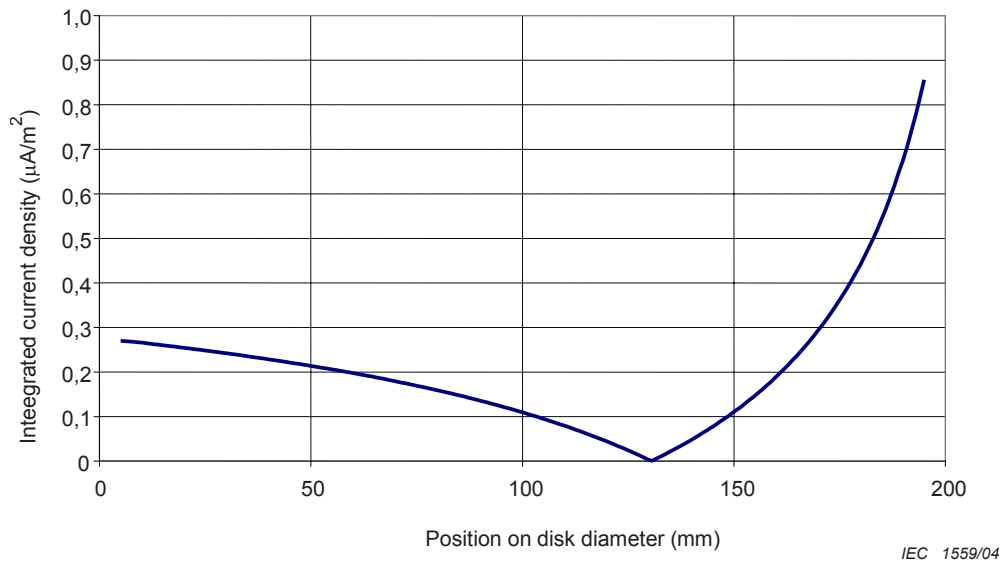


Figure B.4 – Distribution of integrated induced current density along the diameter AA of the disk (source: 1 wire, located at $d = 10$ mm from the edge of the disk)

B.1.1.2 Distance to the source $d = 100$ mm

Results of the computation of local induced currents in the disk are given hereunder in form of graphs giving the shape of the distribution of induced currents in the disk (Figure B.5). The curve in Figure B.6 gives the numerical values of the distribution of the induced currents integrated over a surface of 1 cm^2 perpendicular to the induced current direction.

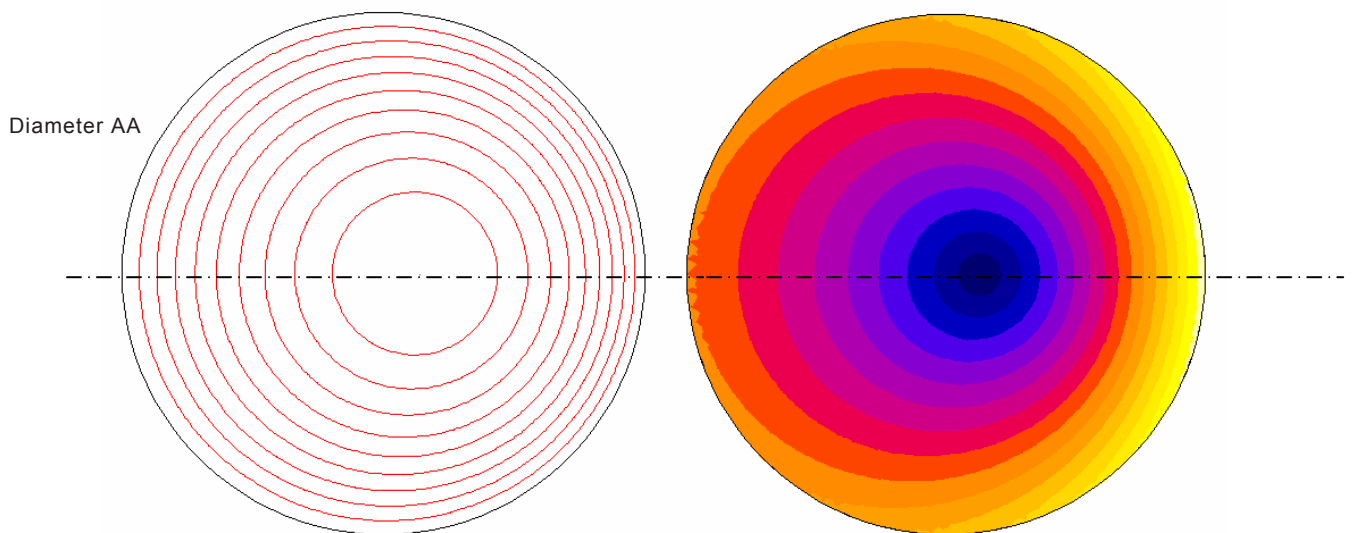


Figure B.5 – Current density lines J and distribution of J in the disk (source: 1 wire, located at $d = 100$ mm from the edge of the disk)

IEC 1560/04

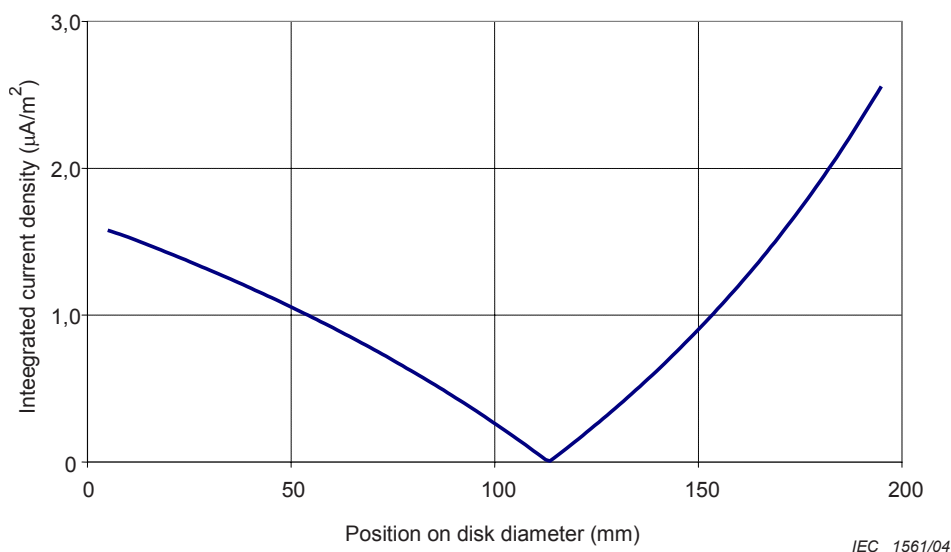


Figure B.6 – Distribution of integrated induced current density along the diameter AA of the disk (source: 1 wire, located at $d = 100$ mm from the edge of the disk)

B.1.1.3 Distance to the source $d = 1\ 000$ mm

Current density lines J , distribution of J in the disk and distribution of induced current density calculated on the diameter of the disk are similar to those computed in the case of a uniform field (Annex A).

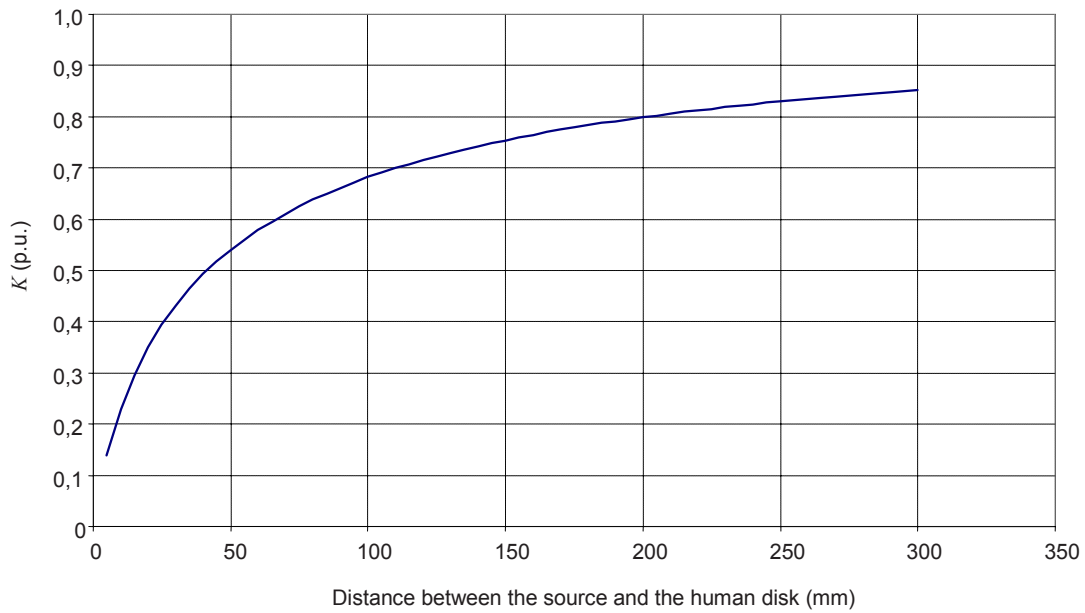
The higher is the distance d between the source and the disk, the lower is the difference with the computation results obtained with the hypothesis of uniform field: in the present case, $J_{i\ max} = 0,353 \times 10^{-5}$ A/m², to be compared to the value calculated with a uniform field ($J_{i\ max} = 0,375 \times 10^{-5}$ A/m²).

B.1.2 Calculated values of the coupling factor for non-uniform magnetic field K

Results of the computation of the coupling factor for non-uniform magnetic field K , as a function of the distance d , are given hereunder in a graphic form (see Figures B.7 and B.8). Corresponding numerical values are given in Tables B.1 and B.2.

The distance d is the minimum distance between the edge of the disk and the closer part of the source.

B.1.2.1 Calculations for short distances to the source: $0 < d < 300$ mm



IEC 1562/04

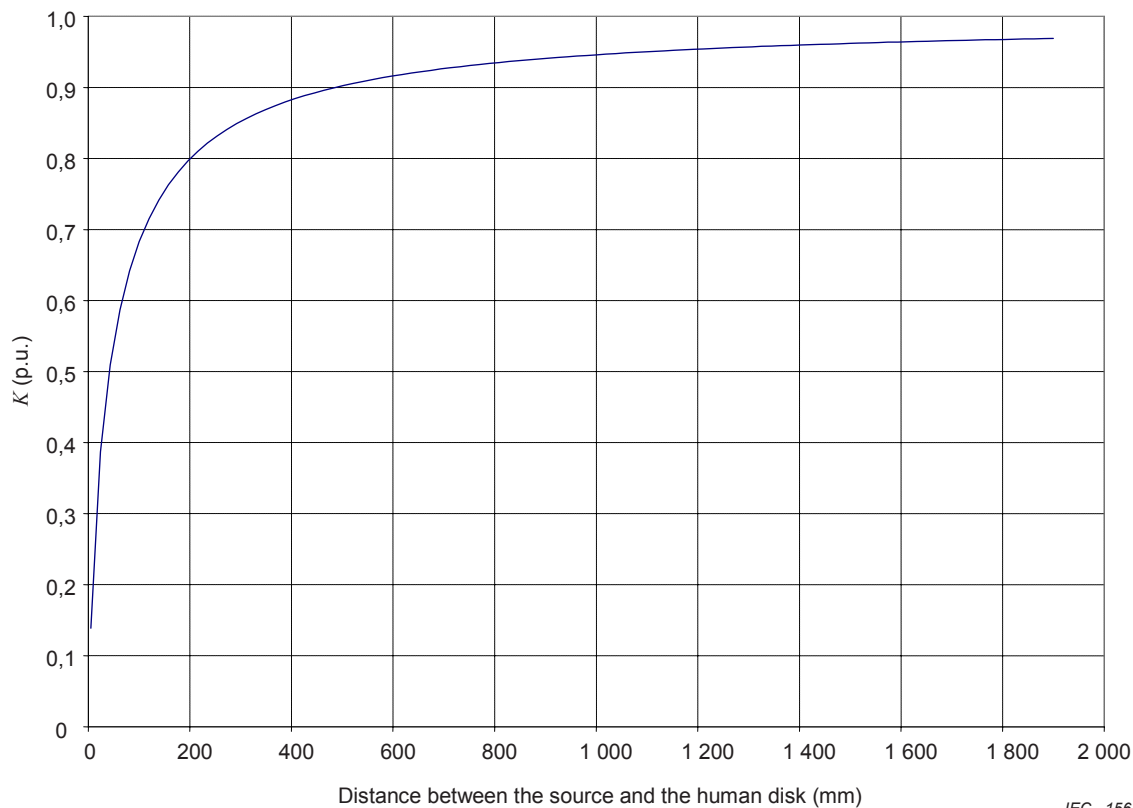
Figure B.7 – Parametric curve of factor K for distances up to 300 mm to a source consisting of an infinitely long wire (disk: $R = 100$ mm)

Table B.1 – Numerical values of factor K for distances up to 300 mm to a source consisting of an infinitely long wire (disk: $R = 100$ mm)

Distance between the source and the disk mm	Coupling factor K
10	0,229
20	0,350
30	0,432
40	0,492
50	0,540
60	0,579
70	0,611
80	0,638
90	0,661
100	0,682

Distance between the source and the disk mm	Coupling factor K
110	0,700
120	0,716
130	0,730
140	0,743
150	0,754
160	0,765
170	0,775
180	0,783
190	0,792
200	0,799

Distance between the source and the disk mm	Coupling factor K
210	0,806
220	0,813
230	0,819
240	0,824
250	0,830
260	0,835
270	0,839
280	0,844
290	0,848
300	0,852

B.1.2.2 Calculations for higher distances: $0 < d < 1\,900$ mm

IEC 1563/04

Figure B.8 – Parametric curve of factor K for distances up to 1 900 mm to a source consisting of an infinitely long wire (disk: $R = 100$ mm)

Table B.2 – Numerical values of factor K for distances up to 1 900 mm to a source consisting of an infinitely long wire (disk: $R = 100$ mm)

Distance between the source and the disk mm	Coupling factor K	Distance between the source and the disk mm	Coupling factor K	Distance between the source and the disk mm	Coupling factor K
5	0,139	656	0,922	1 307	0,957
43	0,509	694	0,926	1 345	0,958
82	0,642	732	0,929	1 383	0,959
120	0,715	771	0,932	1 421	0,960
158	0,763	809	0,935	1 460	0,961
196	0,797	847	0,938	1 498	0,962
235	0,821	886	0,940	1 536	0,963
273	0,841	924	0,942	1 575	0,964
311	0,856	962	0,944	1 613	0,964
350	0,869	1 000	0,946	1 651	0,965
388	0,879	1 039	0,948	1 689	0,966
426	0,888	1 077	0,949	1 728	0,966
464	0,896	1 115	0,951	1 766	0,967
503	0,903	1 153	0,952	1 804	0,968
541	0,908	1 192	0,954	1 843	0,968
579	0,914	1 230	0,955	1 881	0,969
618	0,918	1 268	0,956		

B.2 Calculations for a conductive disk with a radius $R = 200$ mm

Results of the computation of the coupling factor for non-uniform magnetic fields K , as a function of the distance d , are given hereunder in a graphic form (see Figures B.9 and B.10). Corresponding numerical values are given in Tables B.3 and B.4.

The distance d is the minimum distance between the edge of the disk and the closest part of the source.

B.2.1 Calculations for short distances to the source: $0 < d < 300$ mm

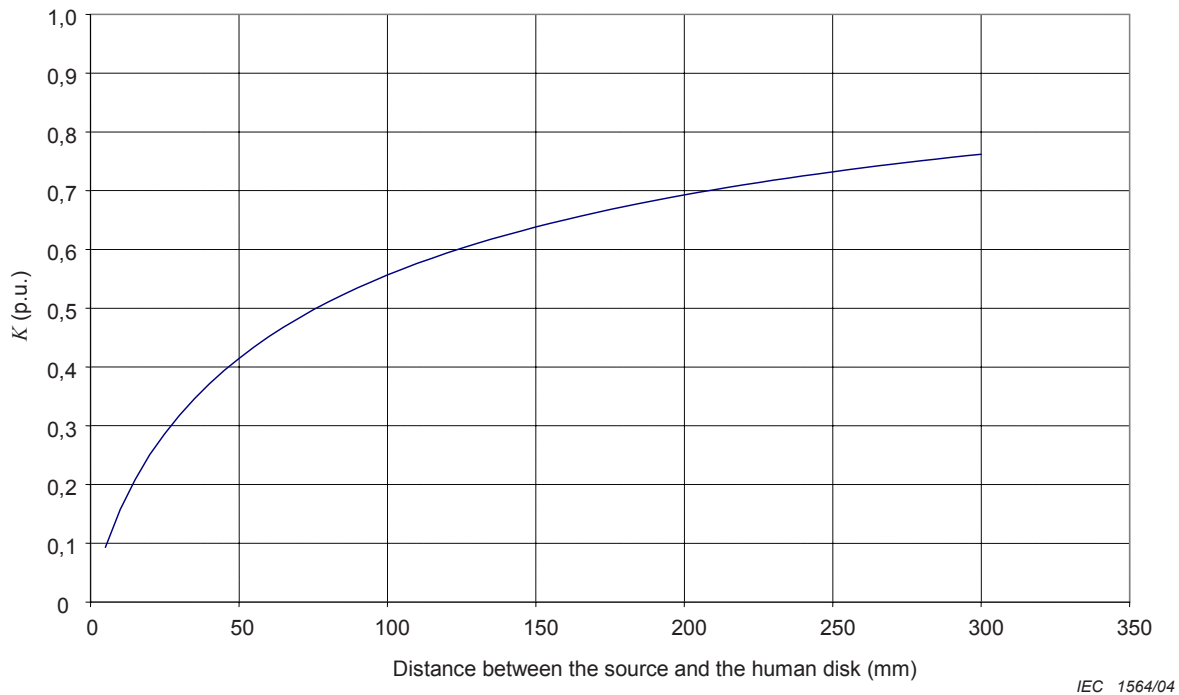


Figure B.9 – Parametric curve of factor K for distances up to 300 mm to a source consisting of an infinitely long wire (disk: $R = 200$ mm)

Table B.3 – Numerical values of factor K for distances up to 300 mm to a source consisting of an infinitely long wire (disk: $R = 200$ mm)

Distance between the source and the disk mm	Coupling factor K
10	0,158
20	0,250
30	0,318
40	0,371
50	0,415
60	0,451
70	0,483
80	0,510
90	0,535
100	0,556

Distance between the source and the disk mm	Coupling factor K
110	0,576
120	0,594
130	0,610
140	0,625
150	0,638
160	0,651
180	0,673
190	0,683
200	0,693

Distance between the source and the disk mm	Coupling factor K
210	0,701
220	0,710
230	0,718
240	0,725
250	0,732
260	0,739
270	0,745
280	0,751
290	0,757
300	0,762

B.2.2 Calculations for higher distances to the source : $0 < d < 1\,900$ mm

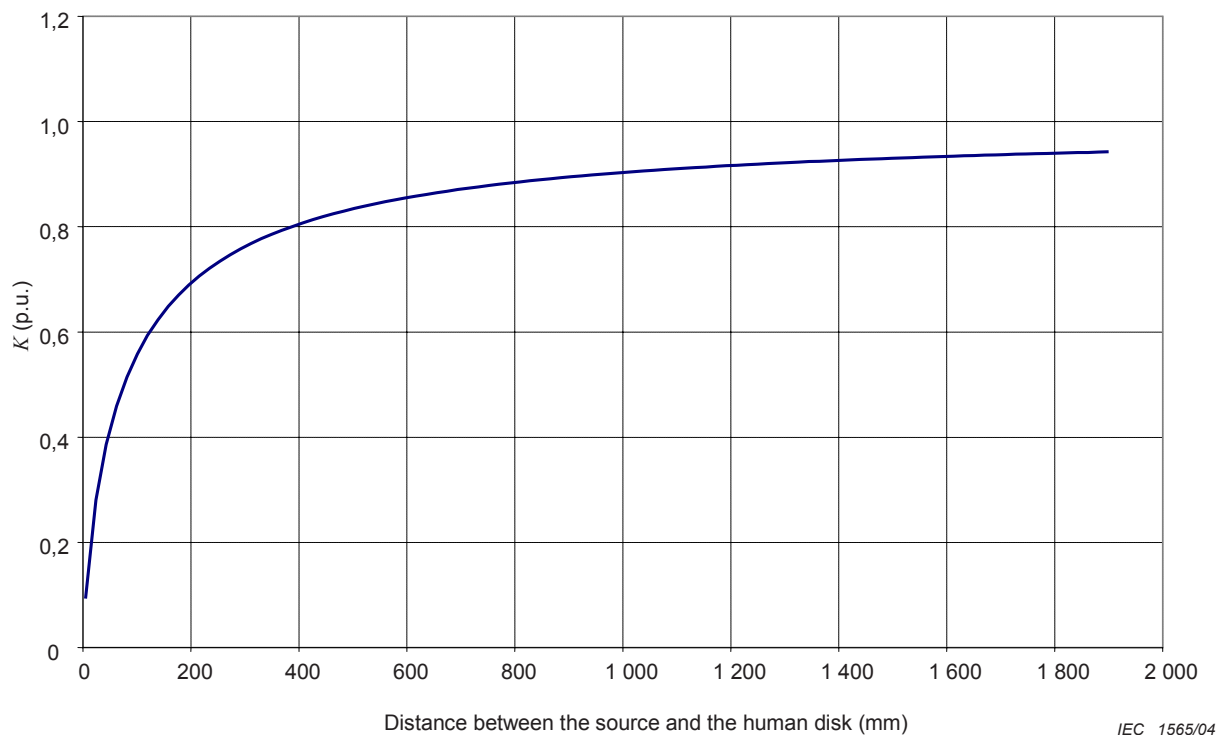


Figure B.10 – Parametric curve of factor K for distances up to 1 900 mm to a source consisting of an infinitely long wire (*disk: $R = 200$ mm*)

Table B.4 – Numerical values of factor K for distances up to 1 900 mm to a source consisting of an infinitely long wire (*disk: $R = 200$ mm*)

Distance between the source and the disk mm	Coupling factor K	Distance between the source and the disk mm	Coupling factor K	Distance between the source and the disk mm	Coupling factor K
43	0,386	771	0,881	1 345	0,924
120	0,593	809	0,885	1 383	0,925
196	0,689	847	0,889	1 421	0,927
273	0,747	886	0,893	1 460	0,929
330	0,777	924	0,897	1 498	0,930
350	0,785	962	0,900	1 536	0,931
369	0,793	1 000	0,903	1 575	0,933
388	0,800	1 039	0,906	1 594	0,933
426	0,813	1 077	0,909	1 651	0,935
464	0,825	1 115	0,911	1 689	0,937
503	0,835	1 153	0,914	1 709	0,937
541	0,843	1 192	0,916	1 766	0,939
579	0,851	1 211	0,917	1 804	0,940
618	0,858	1 230	0,918	1 843	0,941
656	0,865	1 249	0,919	1 881	0,942
694	0,871	1 268	0,920		
732	0,876	1 307	0,922		

Annex C (normative)

Disk in a field created by 2 parallel wires with balanced currents

The induced currents are calculated in a disk of homogeneous conductivity. In order to allow comparison between different field sources configurations (depending on the geometry of the source and distance to the disk) the following standard values have been chosen:

- f , frequency = 50 Hz (see Note 2 in 3.5);
- B , magnetic flux density = $1,25 \mu\text{T}$, at the edge of the disk closer to the field source;
- R , radius of the conductive disk = 100 mm and 200 mm;
- σ , conductivity (homogeneous) = $0,2 \text{ S/m}$.

In this annex, the magnetic field is generated by a set of 2 parallel wires with balanced currents (these straight and infinitely long wires are a simplified representation of an electrical transmission or distribution line). The conductive disk and the field source are located in the same plane, at a distance d , and the 2 wires are separated by a distance e (see Figure C.1).

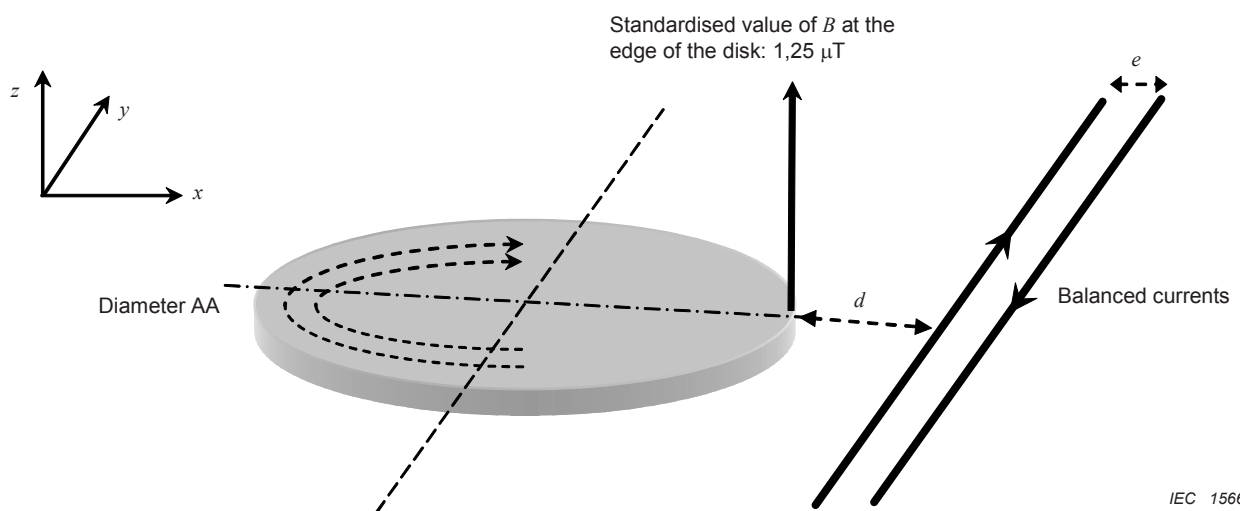
The evolution of the coupling factor for non-uniform magnetic field K is studied with regard to the distance d for:

- exposure close to the source: $0 < d < 300 \text{ mm}$;
- exposure at higher distance $0 < d < 1\,900 \text{ mm}$.

For each distance d , the factor K is calculated for 5 different distances e between the 2 wires: 5 mm, 10 mm, 20 mm, 40 mm and 80 mm.

For illustrations, three results of computation are presented, corresponding to 3 distances d between the disk and the wires ($d = 7,5 \text{ mm}$, $97,5 \text{ mm}$ and 900 mm), and with $e = 5 \text{ mm}$.

NOTE d is the distance between the edge of the disk and the closest part of the source, i.e. the closest wire. Considering the distance between the wires ($e = 5 \text{ mm}$), a value $d = 7,5 \text{ mm}$ corresponds to a distance of 10 mm between the edge of the disk and the median axis of the 2 wires.



IEC 1566/04

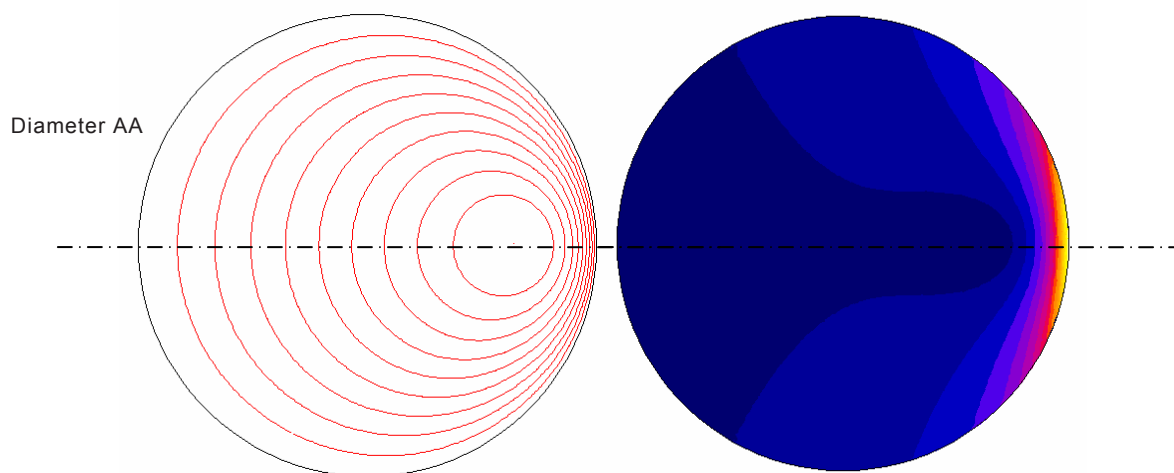
**Figure C.1 – Conductive disk in the magnetic field generated
by 2 parallel wires with balanced currents**

C.1 Calculations for a conductive disk with a radius $R = 100$ mm

C.1.1 Examples of calculation of induced currents in the disk

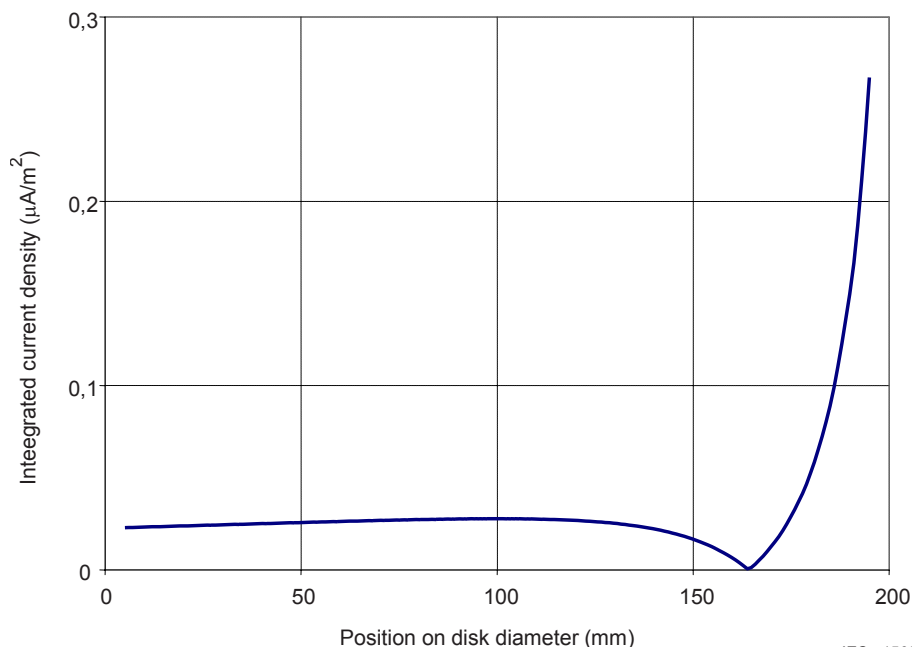
C.1.1.1 Distance to the source $d = 7,5$ mm

Results of the computation of local induced currents in the disk are given hereunder in form of graphs giving the shape of the distribution of induced currents in the disk (Figure C.2). The curve in Figure C.3 gives the numerical values of the distribution of the induced currents integrated over a surface of 1 cm^2 perpendicular to the induced current direction.



IEC 1567/04

Figure C.2 – Current density lines J and distribution of J in the disk
(source: 2 parallel wires with balanced currents, separated by 5 mm, located at $d = 7,5$ mm from the edge of the disk)



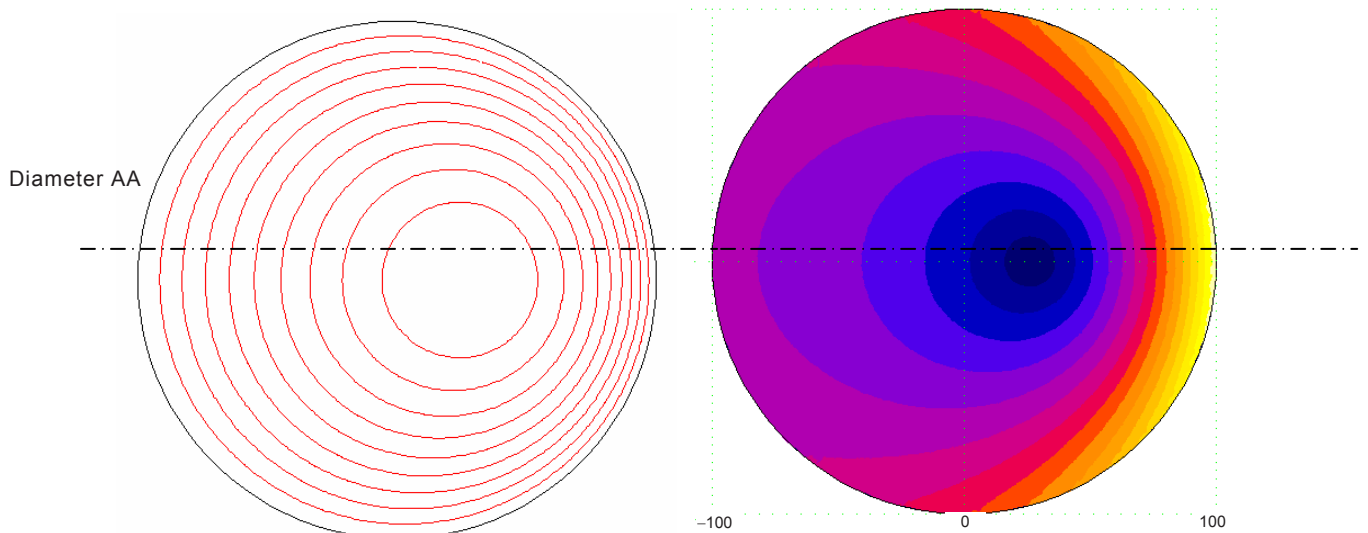
IEC 1568/04

Figure C.3 – $J_i = f[r]$: Distribution of integrated induced current density calculated along the diameter AA of the disk
(source: 2 parallel wires with balanced currents, separated by 5 mm, located at $d = 7,5$ mm from the edge of the disk)

NOTE The diameter AA is located as illustrated in Figures C.1 and C.2.

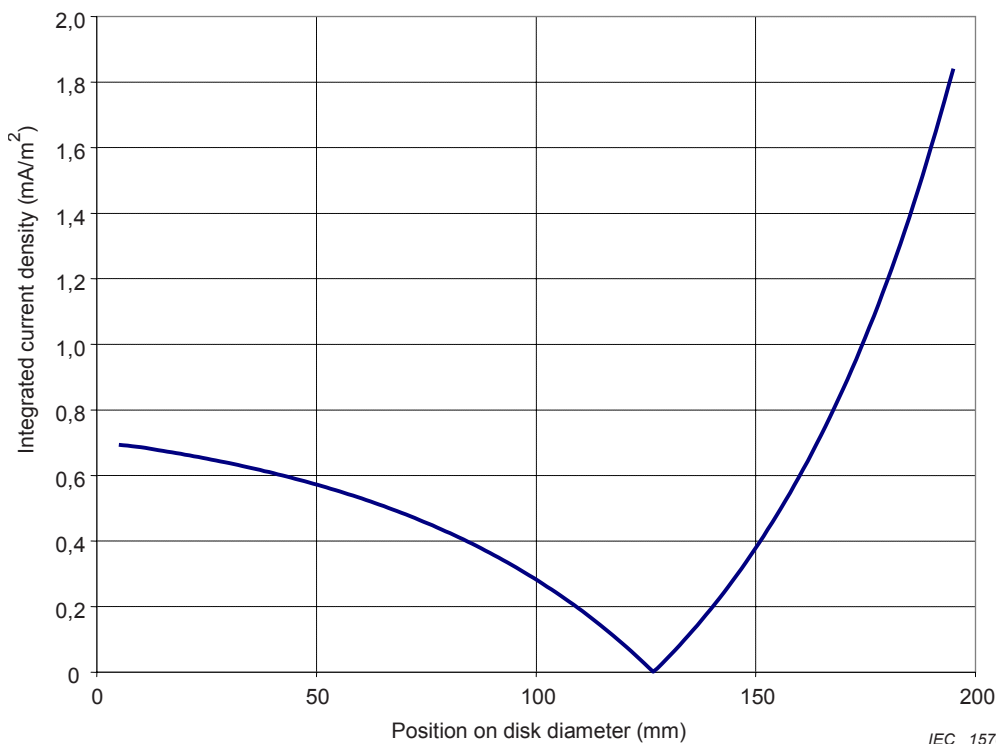
C.1.1.2 Distance to the source $d = 97,5$ mm

Results of the computation of local induced currents in the disk are given hereunder in form of graphs giving the shape of the distribution of induced currents in the disk (Figure C.4). The curve in Figure C.5 gives the numerical values of distribution of the induced currents integrated over a surface of 1 cm^2 perpendicular to the induced current direction.



IEC 1569/04

Figure C.4– Current density lines J and distribution of J in the disk
 (source: 2 parallel wires with balanced currents separated by 5 mm, located at $d = 97,5$ mm from the edge of the disk)



IEC 1570/04

Figure C.5 – $J_i = f [r]$: Distribution of integrated induced current density calculated along the diameter AA of the disk
 (source: 2 parallel wires with balanced currents separated by 5 mm, located at $d = 97,5$ mm from the edge of the disk)

NOTE The diameter AA is located as illustrated in Figures C.1 and C.4.

C.1.1.3 Distance to the source $d = 900$ mm

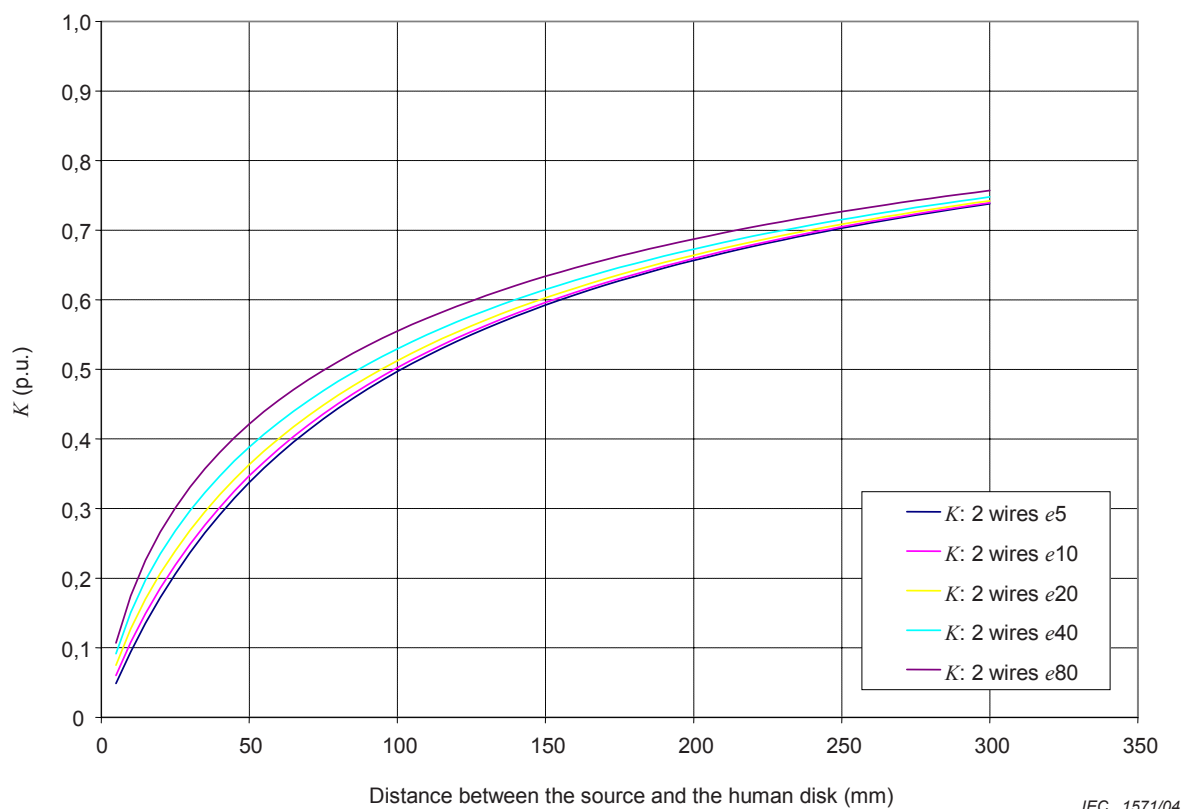
Computation results are similar to the case given in B.1.1.3 (one-wire configuration).

C.1.2 Calculated values of the coupling factor for non-uniform magnetic field K

Results of the computation of the coupling factor for non-uniform magnetic fields K , as a function of the distance d , are given hereunder in form of parametric curves, for different values of distances between the 2 wires (parameter e): see Figures C.6 and C.7. Corresponding numerical values are given in Tables C.1 and C.2.

The distance d is the minimum distance between the edge of the disk and the closest part of the source (i.e. the closest wire).

C.1.2.1 Short distances to the source: $0 < d < 300$ mm



IEC 1571/04

Figure C.6 – Parametric curves of factor K for distances up to 300 mm to a source consisting of 2 parallel wires with balanced currents and for different distances e between the 2 wires (homogeneous disk $R = 100$ mm)

Table C.1 – Numerical values of factor K for distances up to 300 mm to a source consisting of 2 parallel wires with balanced currents (homogeneous disk: $R = 100$ mm)

Distance between the source and the disk mm	Source: 2 parallel wires with balanced currents separated by a distance e				
	$e = 5$ mm	$e = 10$ mm	$e = 20$ mm	$e = 40$ mm	$e = 80$ mm
10	0,094	0,108	0,127	0,151	0,175
20	0,172	0,186	0,207	0,235	0,267
30	0,237	0,249	0,269	0,297	0,331
40	0,291	0,302	0,320	0,347	0,381
50	0,337	0,347	0,363	0,388	0,421
60	0,378	0,386	0,401	0,424	0,456
70	0,413	0,420	0,434	0,455	0,485
80	0,444	0,451	0,463	0,483	0,511
90	0,472	0,478	0,489	0,507	0,534
100	0,497	0,502	0,513	0,530	0,555
110	0,520	0,525	0,534	0,550	0,574
120	0,540	0,545	0,553	0,568	0,591
130	0,559	0,563	0,571	0,585	0,606
140	0,576	0,580	0,588	0,600	0,620
150	0,592	0,596	0,603	0,615	0,634
160	0,607	0,610	0,617	0,628	0,646
170	0,621	0,624	0,630	0,640	0,657
180	0,634	0,636	0,642	0,652	0,668
190	0,645	0,648	0,653	0,663	0,678
200	0,657	0,659	0,664	0,673	0,687
210	0,667	0,669	0,674	0,682	0,696
220	0,677	0,679	0,683	0,691	0,704
230	0,686	0,688	0,692	0,700	0,712
240	0,695	0,697	0,701	0,708	0,720
250	0,703	0,705	0,708	0,715	0,727
260	0,711	0,712	0,716	0,722	0,733
270	0,718	0,720	0,723	0,729	0,740
280	0,725	0,727	0,730	0,736	0,746
290	0,732	0,733	0,736	0,742	0,751
300	0,738	0,739	0,742	0,748	0,757

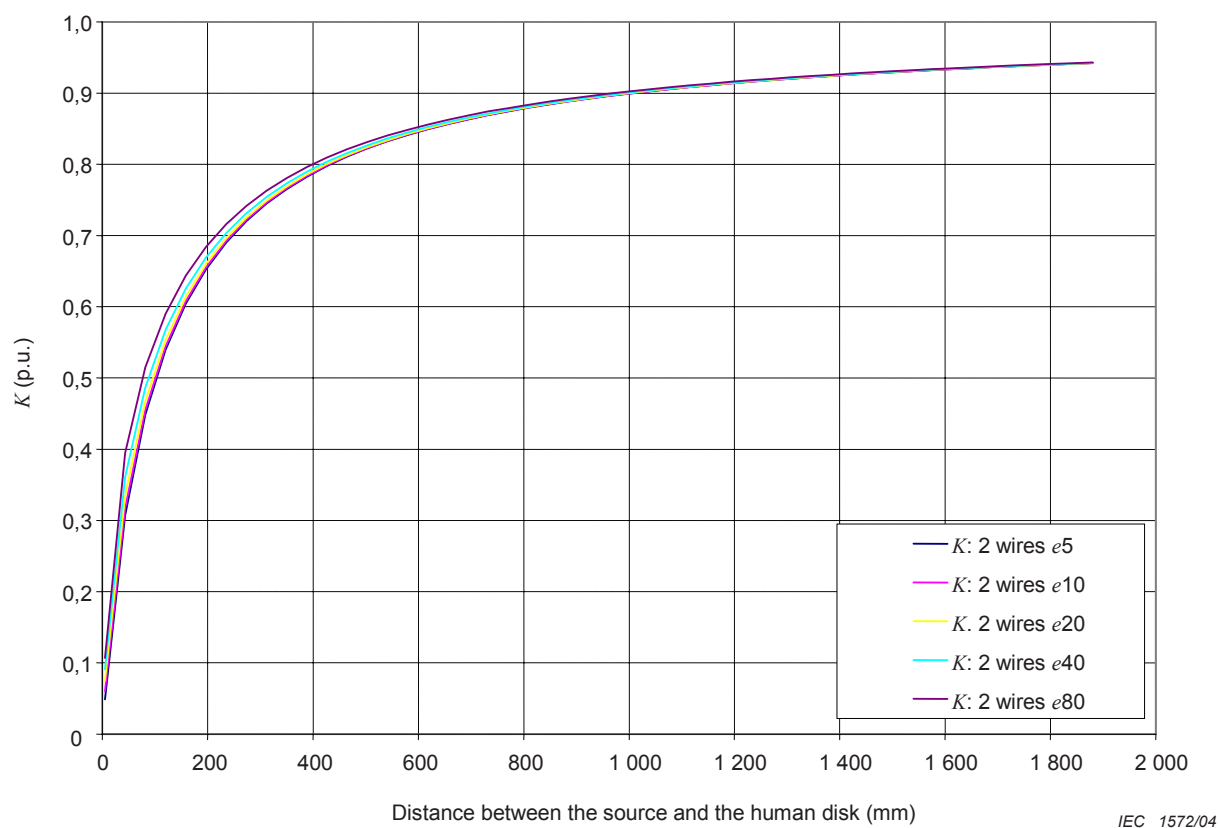
C.1.2.2 Distances to the source: $0 < d < 1\,900$ mm

Figure C.7 – Parametric curves of factor K for distances up to 1 900 mm to a source consisting of 2 parallel wires with balanced currents and for different distances e between the 2 wires (homogeneous disk $R = 100$ mm)

Table C.2 – Numerical values of factor K for distances up to 1 900 mm to a source consisting of 2 parallel wires with balanced currents (homogeneous disk: $R = 100$ mm)

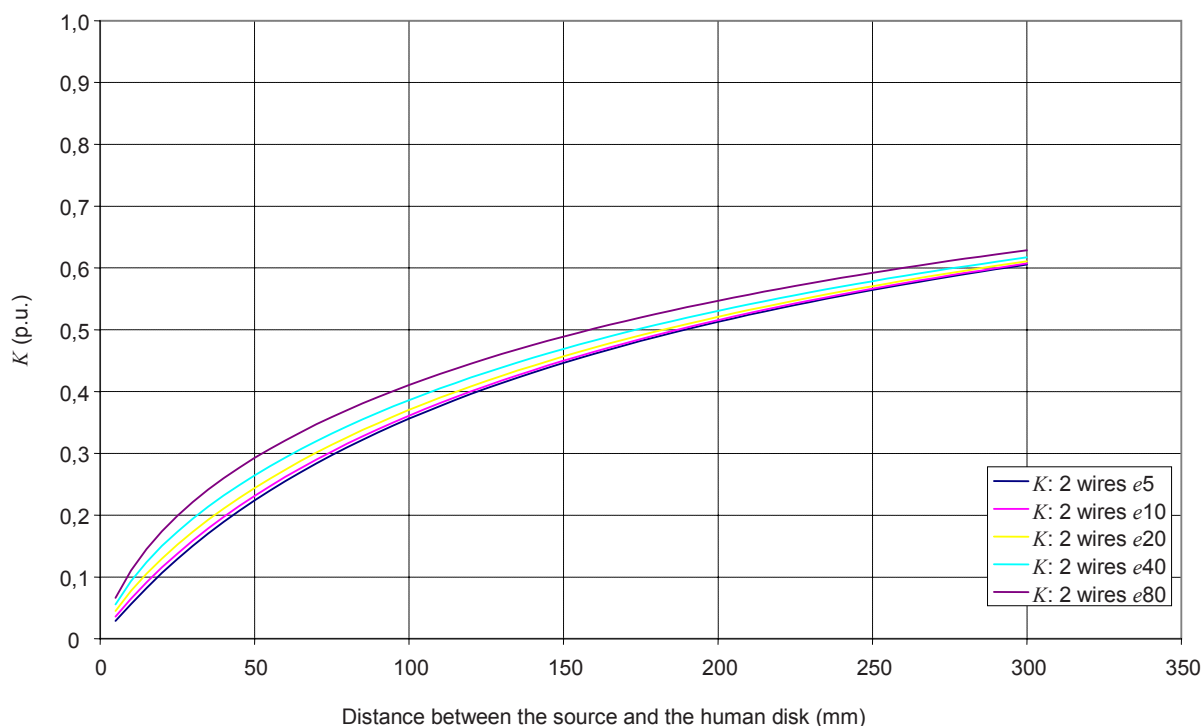
Distance between the source and the disk mm	Source: 2 parallel wires with balanced currents separated by a distance e				
	$e = 5$ mm	$e = 10$ mm	$e = 20$ mm	$e = 40$ mm	$e = 80$ mm
5	0,049	0,060	0,075	0,091	0,107
43	0,307	0,317	0,335	0,361	0,395
82	0,449	0,455	0,467	0,487	0,515
120	0,540	0,545	0,553	0,568	0,590
158	0,604	0,608	0,614	0,626	0,644
196	0,653	0,655	0,660	0,669	0,684
235	0,690	0,692	0,696	0,703	0,716
273	0,720	0,722	0,725	0,731	0,741
311	0,745	0,746	0,749	0,754	0,763
350	0,765	0,766	0,769	0,773	0,781
388	0,783	0,784	0,786	0,789	0,796
426	0,798	0,799	0,800	0,804	0,809
464	0,811	0,811	0,813	0,816	0,821
503	0,822	0,823	0,824	0,827	0,831
541	0,832	0,833	0,834	0,836	0,840
579	0,841	0,842	0,843	0,845	0,848
618	0,849	0,850	0,851	0,852	0,856
656	0,856	0,857	0,858	0,859	0,862
694	0,863	0,863	0,864	0,866	0,868
732	0,869	0,869	0,870	0,871	0,874
771	0,874	0,875	0,875	0,877	0,879
809	0,879	0,880	0,880	0,881	0,884
847	0,884	0,884	0,885	0,886	0,888
886	0,888	0,889	0,889	0,890	0,892
924	0,892	0,892	0,893	0,894	0,896
962	0,896	0,896	0,897	0,897	0,899
1 000	0,899	0,900	0,900	0,901	0,902
1 039	0,903	0,903	0,903	0,904	0,905
1 077	0,906	0,906	0,906	0,907	0,908
1 115	0,908	0,909	0,909	0,910	0,911
1 153	0,911	0,911	0,911	0,912	0,913
1 192	0,913	0,914	0,914	0,915	0,916
1 230	0,916	0,916	0,916	0,917	0,918
1 268	0,918	0,918	0,918	0,919	0,920
1 307	0,920	0,920	0,921	0,921	0,922
1 345	0,922	0,922	0,923	0,923	0,924
1 383	0,924	0,924	0,924	0,925	0,926
1 421	0,926	0,926	0,926	0,927	0,927
1 460	0,928	0,928	0,928	0,928	0,929
1 498	0,929	0,929	0,929	0,930	0,931
1 536	0,931	0,931	0,931	0,931	0,932
1 575	0,932	0,932	0,932	0,933	0,934
1 613	0,934	0,934	0,934	0,934	0,935
1 651	0,935	0,935	0,935	0,936	0,936
1 689	0,936	0,936	0,937	0,937	0,937
1 728	0,938	0,938	0,938	0,938	0,939
1 766	0,939	0,939	0,939	0,939	0,940
1 804	0,940	0,940	0,940	0,940	0,941
1 843	0,941	0,941	0,941	0,941	0,942
1 881	0,942	0,942	0,942	0,942	0,943

C.2 Calculations for a conductive disk with a radius $R = 200$ mm

Results of the computation of the coupling factor for non-uniform magnetic fields K , as a function of the distance d , are given hereunder in form of parametric curves, for different values of distances between the 2 wires (parameter e): see Figures C.8 and C.9. Corresponding numerical values are given in Tables C.3 and C.4.

The distance d is the minimum distance between the edge of the disk and the closest part of the source (i.e. the closest wire).

C.2.1 Calculations for short distances to the source: $0 < d < 300$ mm



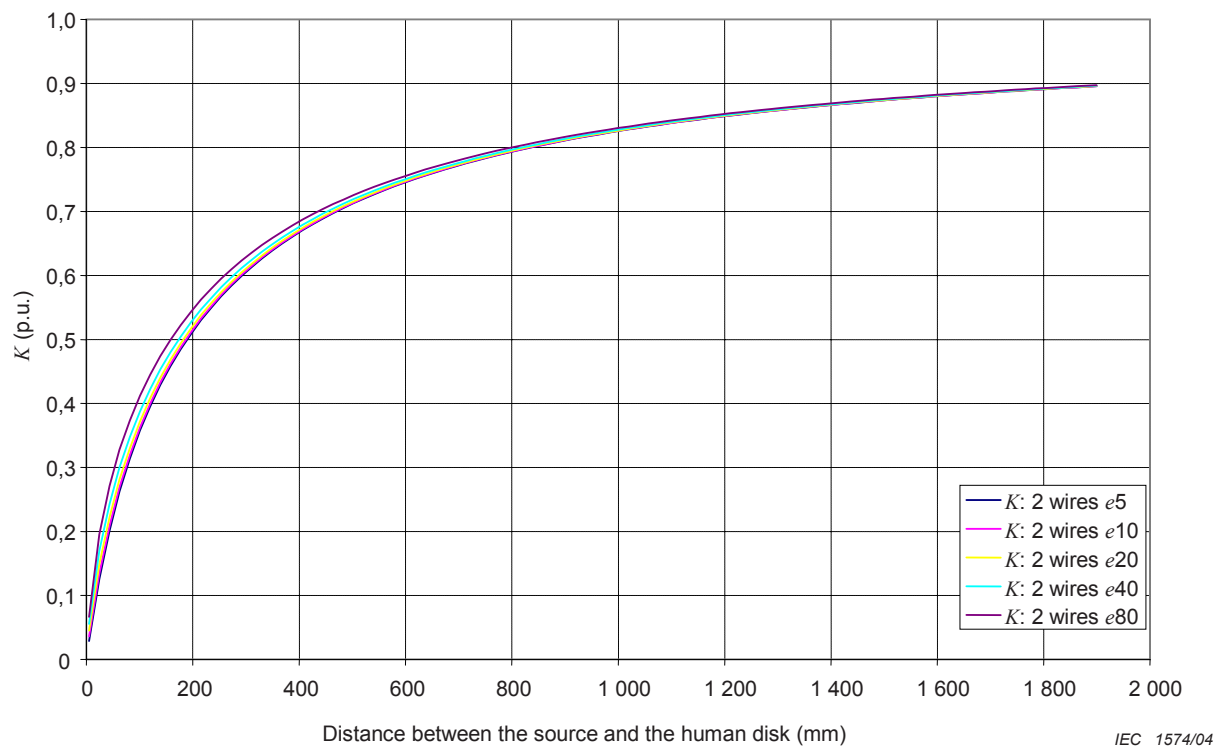
IEC 1573/04

Figure C.8 – Parametric curves of factor K for distances up to 300 mm to a source consisting of 2 parallel wires with balanced currents and for different distances e between the 2 wires (homogeneous disk $R = 200$ mm)

Table C.3 – Numerical values of factor K for distances up to 300 mm to a source consisting of 2 parallel wires with balanced currents (homogeneous disk: $R = 200$ mm)

Source: 2 parallel wires with balanced currents separated by a distance e					
Distance between the source and the disk mm	$e = 5$ mm	$e = 10$ mm	$e = 20$ mm	$e = 40$ mm	$e = 80$ mm
10	0,056	0,065	0,078	0,093	0,111
20	0,106	0,115	0,130	0,150	0,174
30	0,150	0,159	0,173	0,194	0,221
40	0,189	0,197	0,211	0,232	0,260
50	0,224	0,231	0,244	0,264	0,293
60	0,255	0,262	0,274	0,294	0,321
70	0,284	0,290	0,301	0,320	0,347
80	0,310	0,316	0,326	0,344	0,370
90	0,334	0,339	0,349	0,366	0,391
100	0,356	0,361	0,370	0,386	0,411
110	0,377	0,381	0,390	0,405	0,428
120	0,396	0,400	0,408	0,423	0,445
130	0,414	0,418	0,425	0,439	0,461
140	0,430	0,434	0,442	0,454	0,475
150	0,446	0,450	0,457	0,469	0,489
160	0,461	0,465	0,471	0,483	0,502
170	0,475	0,478	0,485	0,496	0,514
180	0,488	0,491	0,497	0,508	0,526
190	0,501	0,504	0,509	0,520	0,537
200	0,513	0,516	0,521	0,531	0,547
210	0,524	0,527	0,532	0,541	0,557
220	0,535	0,537	0,542	0,551	0,566
230	0,545	0,548	0,552	0,561	0,575
240	0,555	0,557	0,562	0,570	0,584
250	0,564	0,566	0,571	0,579	0,592
260	0,573	0,575	0,579	0,587	0,600
270	0,582	0,584	0,588	0,595	0,608
280	0,590	0,592	0,596	0,603	0,615
290	0,598	0,600	0,603	0,610	0,622
300	0,605	0,607	0,611	0,617	0,629

C.2.2 Calculations for higher distances $0 < d < 1\,900$ mm



IEC 1574/04

Figure C.9 – Parametric curves of factor K for distances up to 1 900 mm to a source consisting of 2 parallel wires with balanced currents and for different distances e between the 2 wires (homogeneous disk $R = 200$ mm)

Table C.4 – Numerical values of factor K for distances up to 1 900 mm to a source consisting of 2 parallel wires with balanced currents (homogeneous disk: $R = 200$ mm)

Source: 2 parallel wires with balanced currents separated by a distance e					
Distance between the source and the disk mm	$e = 5$ mm	$e = 10$ mm	$e = 20$ mm	$e = 40$ mm	$e = 80$ mm
5	0,029	0,036	0,045	0,056	0,066
43	0,201	0,209	0,222	0,243	0,271
82	0,314	0,319	0,330	0,347	0,373
120	0,395	0,400	0,408	0,422	0,445
158	0,458	0,462	0,468	0,480	0,499
196	0,509	0,511	0,517	0,527	0,543
235	0,550	0,552	0,557	0,565	0,579
273	0,584	0,586	0,590	0,597	0,610
311	0,614	0,615	0,619	0,625	0,636
350	0,639	0,640	0,643	0,649	0,659
388	0,661	0,662	0,665	0,670	0,678
426	0,680	0,682	0,684	0,688	0,696
464	0,698	0,699	0,701	0,705	0,712
503	0,713	0,714	0,716	0,719	0,726
522	0,720	0,721	0,723	0,726	0,732
541	0,727	0,728	0,729	0,733	0,738
579	0,739	0,740	0,742	0,745	0,750
618	0,751	0,751	0,753	0,756	0,760
656	0,761	0,762	0,763	0,766	0,770
694	0,771	0,771	0,772	0,775	0,779
732	0,780	0,780	0,781	0,783	0,787
771	0,788	0,788	0,789	0,791	0,795
790	0,791	0,792	0,793	0,795	0,798
809	0,795	0,796	0,796	0,798	0,802
847	0,802	0,803	0,803	0,805	0,808
886	0,809	0,809	0,810	0,811	0,814
924	0,815	0,815	0,816	0,817	0,820
962	0,820	0,821	0,821	0,823	0,825
1 000	0,826	0,826	0,827	0,828	0,830
1 039	0,831	0,831	0,832	0,833	0,835
1 077	0,835	0,836	0,836	0,837	0,840
1 115	0,840	0,840	0,841	0,842	0,844
1 153	0,844	0,844	0,845	0,846	0,848
1 192	0,848	0,848	0,849	0,850	0,852
1 230	0,852	0,852	0,852	0,853	0,855
1 268	0,855	0,856	0,856	0,857	0,859
1 307	0,859	0,859	0,859	0,860	0,862
1 345	0,862	0,862	0,863	0,863	0,865
1 383	0,865	0,865	0,866	0,866	0,868
1 421	0,868	0,868	0,869	0,869	0,871
1 460	0,871	0,871	0,871	0,872	0,873
1 498	0,873	0,874	0,874	0,875	0,876
1 536	0,876	0,876	0,876	0,877	0,878
1 575	0,878	0,879	0,879	0,880	0,881
1 613	0,881	0,881	0,881	0,882	0,883
1 651	0,883	0,883	0,884	0,884	0,885
1 689	0,885	0,885	0,886	0,886	0,887
1 709	0,886	0,886	0,887	0,887	0,888
1 728	0,887	0,887	0,888	0,888	0,889
1 766	0,889	0,889	0,890	0,890	0,891
1 804	0,891	0,891	0,892	0,892	0,893
1 843	0,893	0,893	0,894	0,894	0,895
1 881	0,895	0,895	0,895	0,896	0,897

Annex D (normative)

Disk in a magnetic field created by a circular coil

The induced currents are calculated in a disk of homogeneous conductivity. In order to allow comparison between different field sources configurations (depending on geometry of the source and distance to the disk) the following standard values have been chosen:

- f , frequency = 50 Hz (see note 2 in 3.5);
- B , magnetic flux density = $1,25 \mu\text{T}$, at the edge of the disk closer to the field source;
- R , radius of the conductive disk = 100 mm and 200 mm;
- σ , conductivity (homogeneous) = $0,2 \text{ S/m}$.

In this annex, the magnetic field is generated by an alternating current flowing through a circular coil (simplified representation of a localized source). The conductive disk and the coil are located in the same plane, at a distance d (see Figure D.1).

The distance d is the minimum distance between the edge of the disk and the closer part of the source.

The evolution of the coupling factor for non-uniform magnetic field K is studied with regard to the distance d for:

- exposure close to the source: $0 < d < 300 \text{ mm}$;
- exposure at higher distance: $0 < d < 1\,900 \text{ mm}$.

For each distance d , the factor K is calculated for different sources (i.e. different coil radius: $r = 2,5 \text{ mm}$, 5 mm , 10 mm , 20 mm , 40 mm , 80 mm and 160 mm).

For illustration of induced currents computations, 2 distances are studied ($d = 5 \text{ mm}$ and 850 mm) with different values of the coil radius ($r = 10 \text{ mm}$, 50 mm and 200 mm).

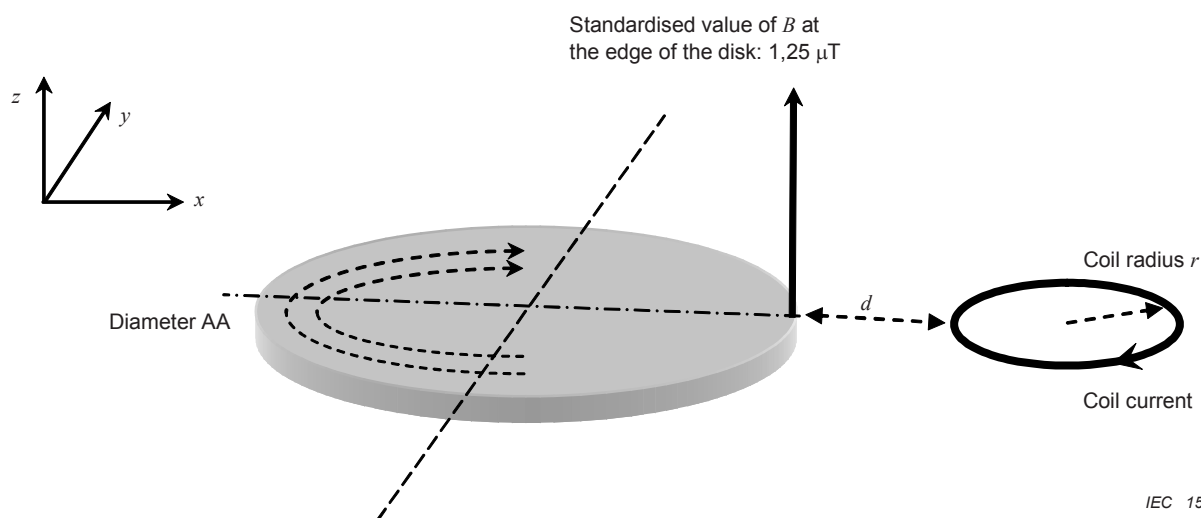


Figure D.1 – Conductive disk in a magnetic field created by a coil

D.1 Calculations for a conductive disk with a radius $R = 100$ mm

D.1.1 Examples of calculation of induced currents in the disk

D.1.1.1 Coil radius $r = 50$ mm, $d = 5$ mm

Results of the computation of local induced currents in the disk are given hereunder in form of graphs giving the shape of the distribution of induced currents in the disk (Figure D.2). The curve in Figure D.3 gives the numerical values of the distribution of the induced currents integrated over a surface of 1 cm^2 perpendicular to the induced current direction.

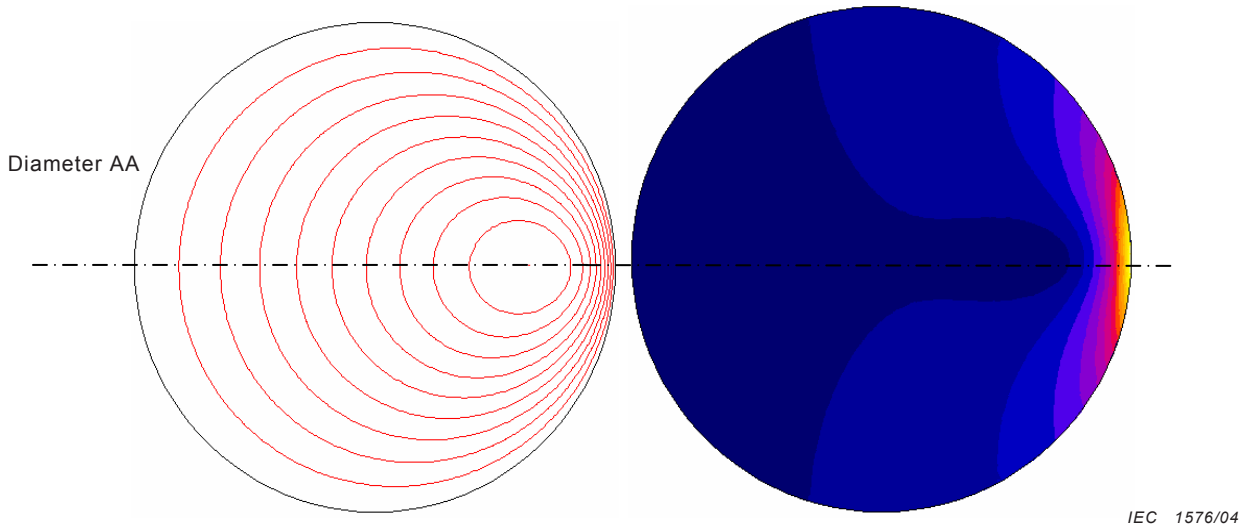


Figure D.2 – Current density lines J and distribution of J in the disk
 (source: coil of radius $r = 50$ mm, conductive disk $R = 100$ mm, $d = 5$ mm)

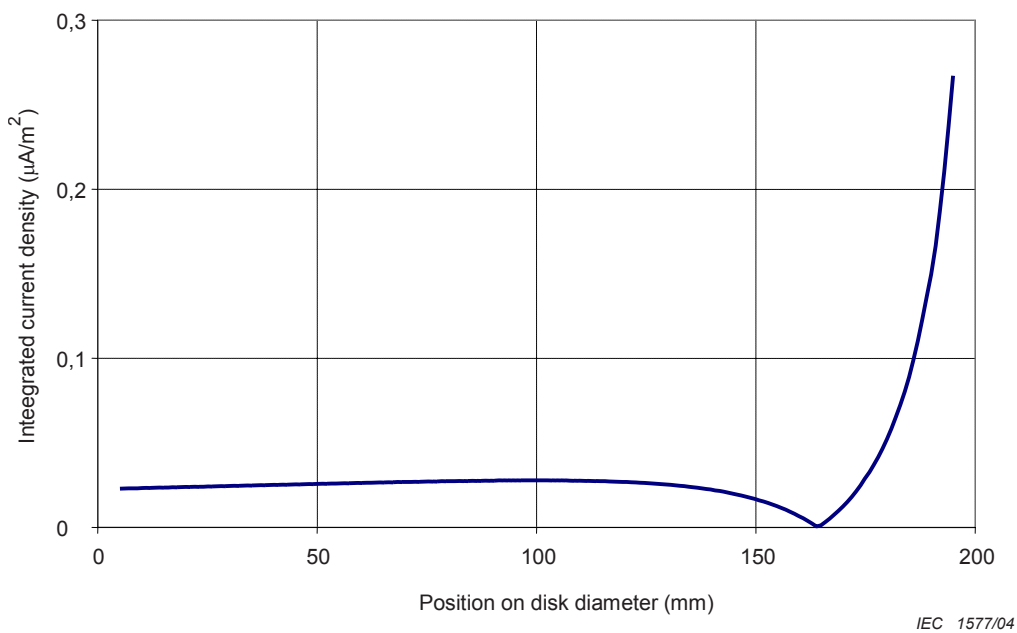


Figure D.3 – $J_i = f [r]$: Distribution of integrated induced current density calculated along the diameter AA of the disk
 (source: coil of radius $r = 50$ mm, conductive disk $R = 100$ mm, $d = 5$ mm)

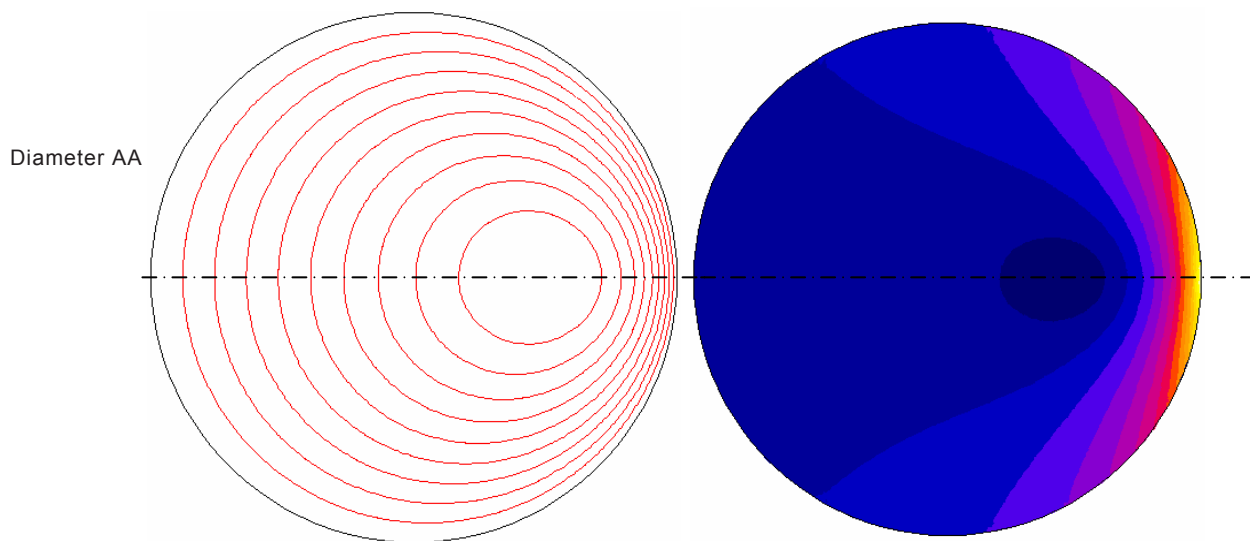
NOTE The diameter AA is located as illustrated in Figures D.1 and D.2.

D.1.1.2 Coil radius $r = 50$ mm, $d = 850$ mm

Results similar to those given in Annexes B and C for high values of d , and so, also similar to the case of the uniform field (Annex A).

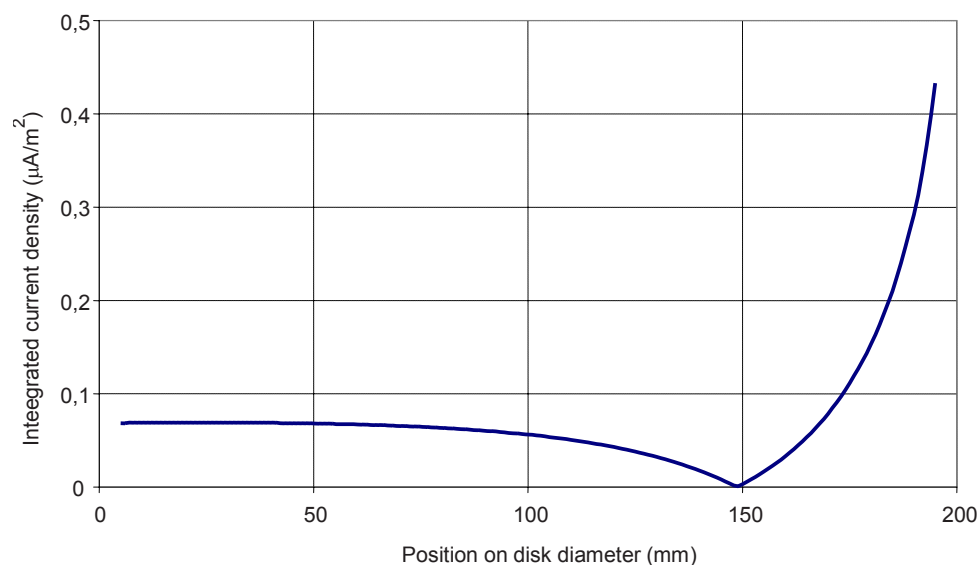
D.1.1.3 Coil radius $r = 200$ mm, $d = 5$ mm

Results of the computation of local induced currents in the disk are given hereunder in form of graphs giving the shape of the distribution of induced currents in the disk (Figure D.4). The curve in Figure D.5 gives the numerical values of the distribution of the induced currents integrated over a surface of 1 cm^2 perpendicular to the induced current direction.



IEC 1578/04

Figure D.4 – Current density lines J and distribution of J in the disk
(source: coil of radius $r = 200$ mm, conductive disk $R = 100$ mm, $d = 5$ mm)



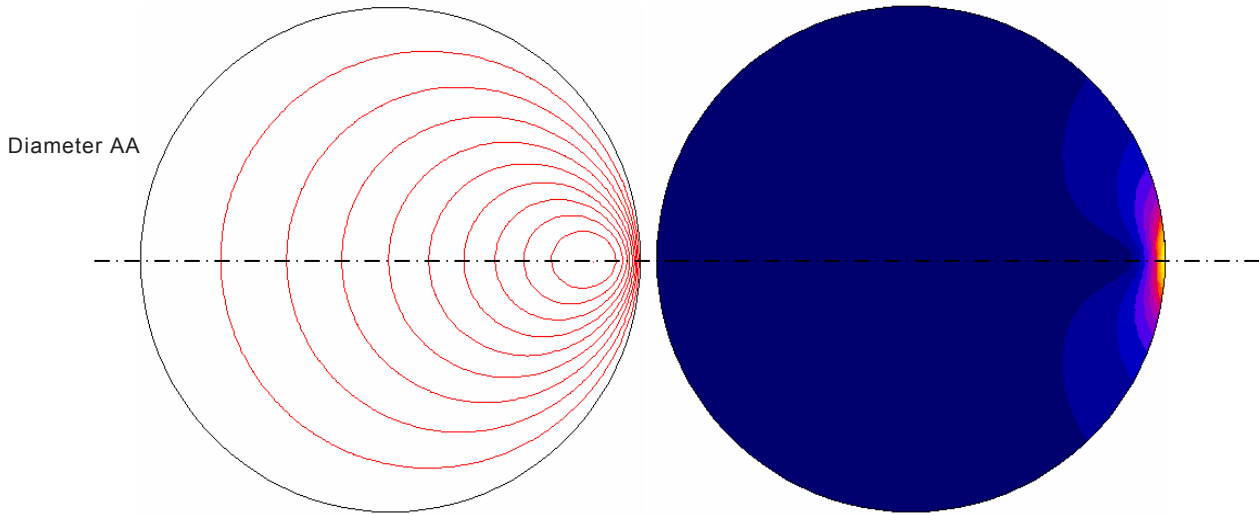
IEC 1579/04

Figure D.5 – $J_i = f[r]$: Distribution of integrated induced current density calculated along the diameter AA of the disk
(source: coil of radius $r = 200$ mm, conductive disk $R = 100$ mm, $d = 5$ mm)

NOTE The diameter AA is located as illustrated in Figures D.1 and D.4.

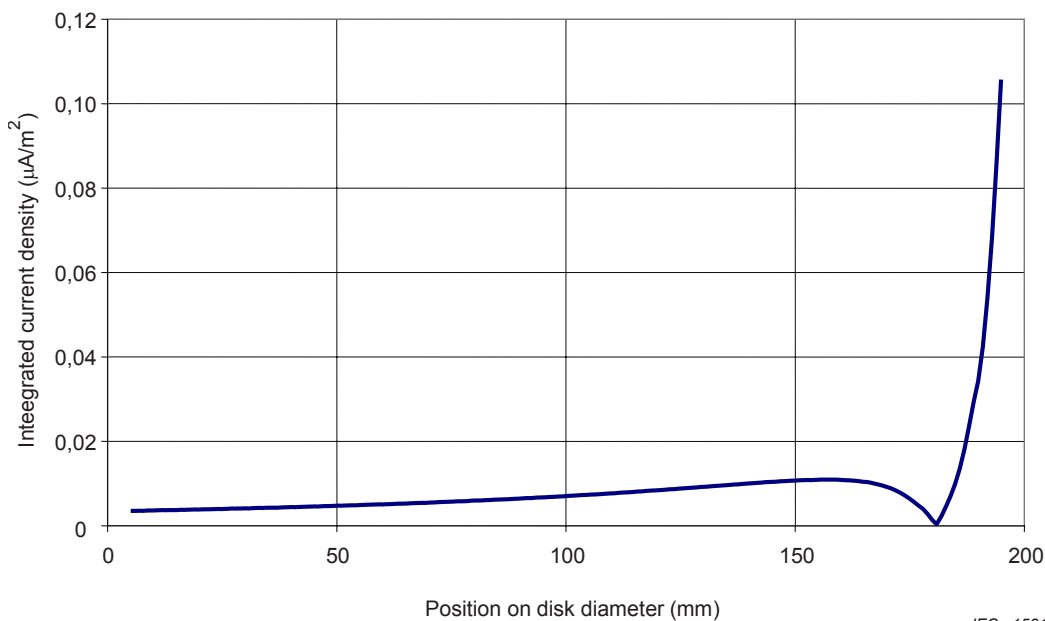
D.1.1.4 Coil radius = 10 mm, $d = 5$ mm

Results of the computation of local induced currents in the disk are given hereunder in form of graphs giving the shape of the distribution of induced currents in the disk (Figure D.6). The curve in Figure D.7 gives the numerical values of the distribution of the induced currents integrated over a surface of 1 cm² perpendicular to the induced current direction.



IEC 1580/04

Figure D.6 – Current density lines J and distribution of J in the disk
 (source: coil of radius $r = 10$ mm, conductive disk $R = 100$ mm, $d = 5$ mm)



IEC 1581/04

Figure D.7 – $J_i = f[r]$: Distribution of integrated induced current density
 calculated along the diameter AA of the disk
 (source: coil of radius $r = 10$ mm, conductive disk $R = 100$ mm, $d = 5$ mm)

NOTE The diameter AA is located as illustrated in Figures D.1 and D.6.

D.1.2 Calculated values of the coupling factor for non-uniform magnetic field K

Results of the computation of the coupling factor for non-uniform magnetic fields K , as a function of the distance d , are given hereunder in the form of parametric curves, for different values of the radius of the source (parameter r , see Figures D.8 and D.9). Corresponding numerical values are given in Tables D.1 and D.2.

The distance d is the minimum distance between the edge of the disk and the closest part of the source.

D.1.2.1 Exposure close to the source: $0 < d < 300$ mm, $R = 100$ mm

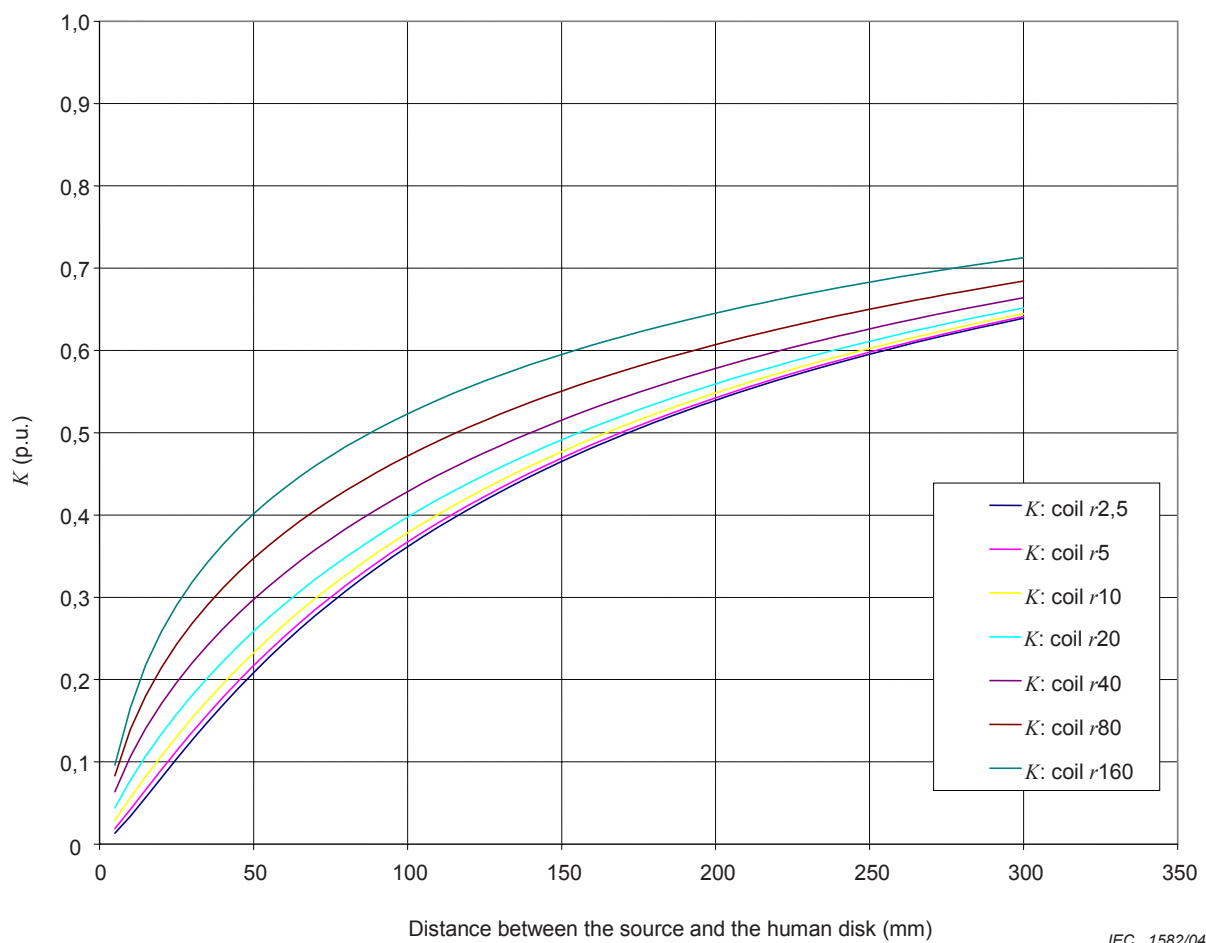


Figure D. 8 – Parametric curves of factor K for distances up to 300 mm to a source consisting of a coil and for different coil radius r (homogeneous disk $R = 100$ mm)

Table D.1 – Numerical values of factor K for distances up to 300 mm to a source consisting of a coil (homogeneous disk: $R = 100$ mm)

Distance between the source and the disk mm	Value of the coil radius mm						
	2,5	5	10	20	40	80	160
10	0,034	0,042	0,056	0,078	0,106	0,139	0,166
20	0,080	0,090	0,107	0,134	0,170	0,214	0,258
30	0,126	0,136	0,153	0,181	0,220	0,268	0,318
40	0,169	0,178	0,195	0,222	0,261	0,311	0,364
50	0,208	0,217	0,233	0,259	0,297	0,347	0,401
60	0,244	0,252	0,267	0,292	0,329	0,378	0,433
70	0,277	0,285	0,298	0,322	0,358	0,405	0,460
80	0,308	0,315	0,327	0,349	0,383	0,430	0,483
90	0,336	0,342	0,354	0,374	0,407	0,452	0,504
100	0,361	0,367	0,378	0,397	0,428	0,472	0,523
110	0,385	0,391	0,401	0,419	0,448	0,490	0,540
120	0,407	0,412	0,422	0,439	0,467	0,507	0,555
130	0,428	0,433	0,442	0,458	0,484	0,523	0,570
140	0,447	0,451	0,460	0,475	0,500	0,537	0,583
150	0,465	0,469	0,477	0,491	0,515	0,551	0,595
160	0,482	0,486	0,493	0,507	0,529	0,563	0,606
170	0,497	0,501	0,508	0,521	0,543	0,575	0,617
180	0,512	0,516	0,522	0,534	0,555	0,586	0,627
190	0,526	0,529	0,536	0,547	0,567	0,597	0,636
200	0,539	0,542	0,548	0,559	0,578	0,607	0,645
210	0,552	0,555	0,560	0,571	0,589	0,617	0,654
220	0,563	0,566	0,572	0,582	0,599	0,626	0,662
230	0,575	0,577	0,582	0,592	0,608	0,634	0,669
240	0,585	0,588	0,593	0,602	0,617	0,642	0,676
250	0,595	0,598	0,602	0,611	0,626	0,650	0,683
260	0,605	0,607	0,612	0,620	0,634	0,658	0,689
270	0,614	0,616	0,620	0,628	0,642	0,665	0,696
280	0,623	0,625	0,629	0,636	0,650	0,671	0,702
290	0,631	0,633	0,637	0,644	0,657	0,678	0,707
300	0,639	0,641	0,645	0,652	0,664	0,684	0,713

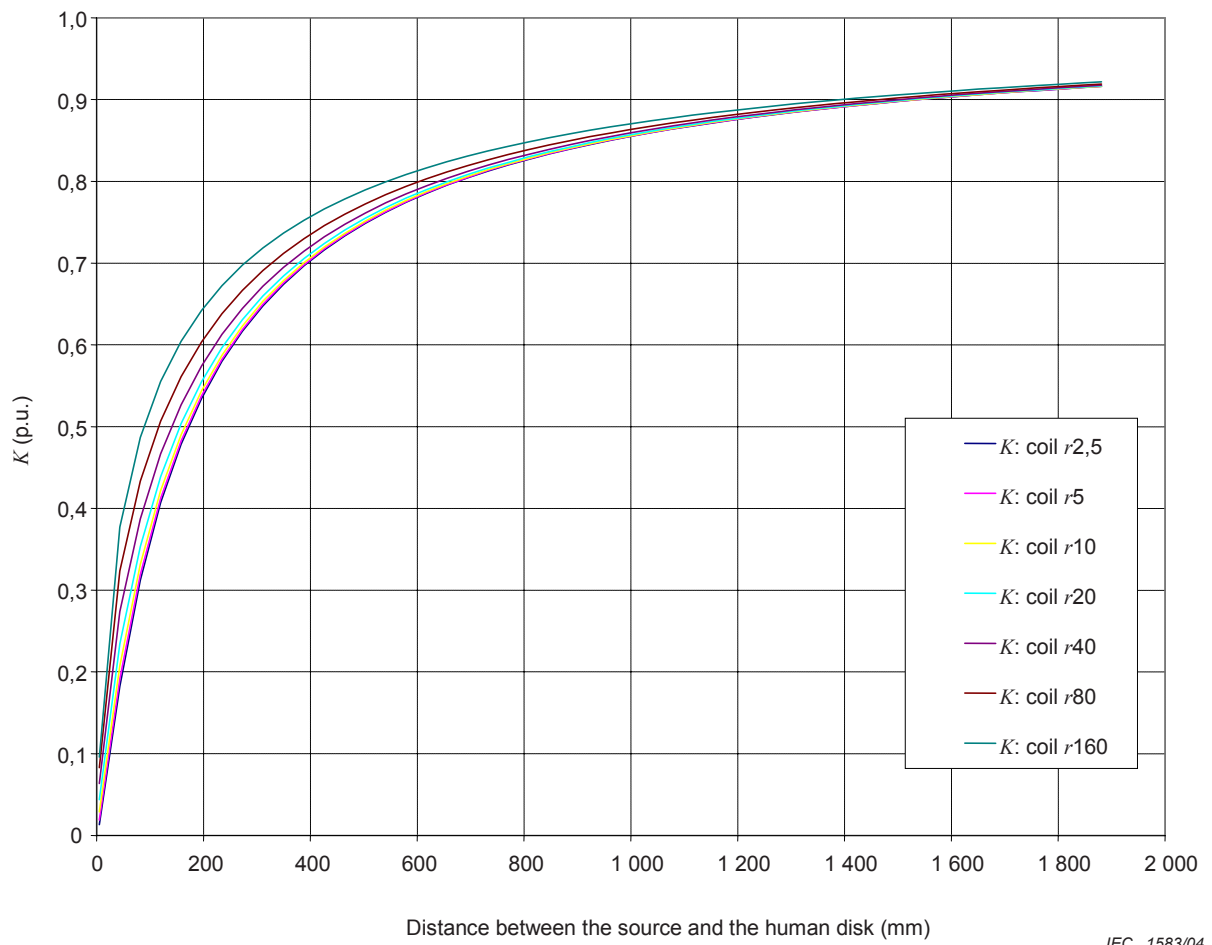
D.1.2.2 Exposure at distance: $0 < d < 1\,900$ mm, $R = 100$ mm

Figure D.9 – Parametric curves of factor K for distances up to 1 900 mm to a source consisting of a coil and for different coil radius r (homogeneous disk $R = 100$ mm)

Table D.2 – Numerical values of factor K for distances up to 1 900 mm to a source consisting of a coil (homogeneous disk: $R = 100$ mm)

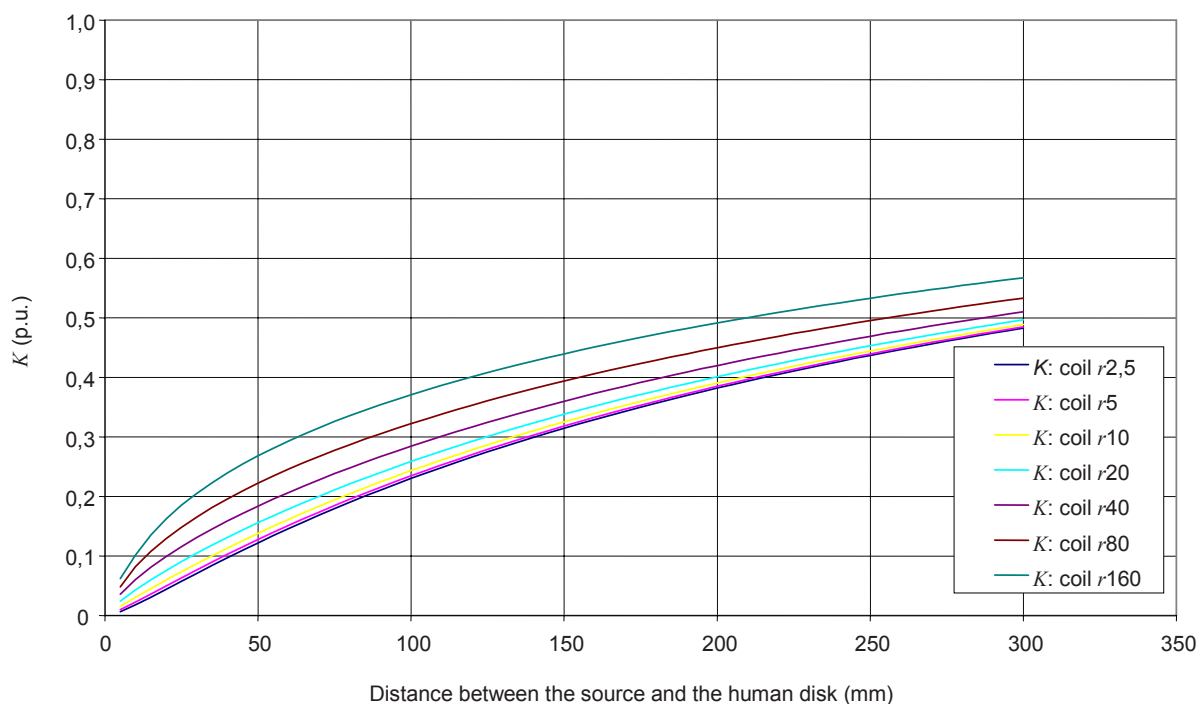
Distance between the source and the disk mm	Value of the coil radius mm						
	2,5	5	10	20	40	80	160
5	0,013	0,019	0,029	0,044	0,064	0,083	0,096
43	0,182	0,191	0,208	0,234	0,274	0,324	0,377
82	0,312	0,319	0,331	0,353	0,387	0,433	0,487
120	0,407	0,412	0,422	0,439	0,467	0,507	0,555
158	0,479	0,483	0,490	0,504	0,527	0,561	0,604
196	0,535	0,538	0,544	0,555	0,574	0,604	0,642
235	0,580	0,582	0,587	0,597	0,613	0,638	0,672
273	0,617	0,619	0,623	0,631	0,645	0,667	0,697
311	0,648	0,650	0,653	0,660	0,672	0,691	0,719
350	0,674	0,676	0,679	0,684	0,695	0,712	0,737
388	0,697	0,698	0,701	0,706	0,715	0,730	0,752
426	0,716	0,717	0,720	0,724	0,732	0,746	0,766
464	0,733	0,734	0,737	0,740	0,748	0,760	0,778
503	0,749	0,750	0,751	0,755	0,761	0,772	0,789
541	0,762	0,763	0,765	0,768	0,774	0,784	0,799
579	0,774	0,775	0,777	0,779	0,785	0,794	0,808
618	0,785	0,786	0,787	0,790	0,795	0,803	0,816
656	0,795	0,796	0,797	0,799	0,804	0,811	0,824
694	0,804	0,805	0,806	0,808	0,812	0,819	0,831
732	0,812	0,813	0,814	0,816	0,820	0,826	0,837
771	0,820	0,821	0,821	0,823	0,827	0,833	0,843
809	0,827	0,827	0,828	0,830	0,833	0,839	0,848
847	0,834	0,834	0,835	0,836	0,839	0,844	0,853
886	0,839	0,840	0,841	0,842	0,845	0,850	0,858
924	0,845	0,845	0,846	0,847	0,850	0,855	0,862
962	0,850	0,850	0,851	0,852	0,855	0,859	0,867
1 000	0,855	0,855	0,856	0,857	0,859	0,863	0,870
1 039	0,860	0,860	0,860	0,861	0,864	0,867	0,874
1 077	0,864	0,864	0,865	0,866	0,868	0,871	0,878
1 115	0,868	0,868	0,869	0,869	0,871	0,875	0,881
1 153	0,872	0,872	0,872	0,873	0,875	0,878	0,884
1 192	0,875	0,875	0,876	0,877	0,878	0,881	0,887
1 230	0,878	0,879	0,879	0,880	0,881	0,884	0,890
1 268	0,882	0,882	0,882	0,883	0,884	0,887	0,892
1 307	0,885	0,885	0,885	0,886	0,887	0,890	0,895
1 345	0,887	0,888	0,888	0,889	0,890	0,893	0,897
1 383	0,890	0,890	0,891	0,891	0,893	0,895	0,899
1 421	0,893	0,893	0,893	0,894	0,895	0,897	0,901
1 460	0,895	0,895	0,896	0,896	0,897	0,900	0,904
1 498	0,898	0,898	0,898	0,899	0,900	0,902	0,906
1 536	0,900	0,900	0,900	0,901	0,902	0,904	0,907
1 575	0,902	0,902	0,902	0,903	0,904	0,906	0,909
1 613	0,904	0,904	0,904	0,905	0,906	0,908	0,911
1 651	0,906	0,906	0,906	0,907	0,908	0,909	0,913
1 689	0,908	0,908	0,908	0,909	0,910	0,911	0,914
1 728	0,910	0,910	0,910	0,910	0,911	0,913	0,916
1 766	0,911	0,911	0,912	0,912	0,913	0,914	0,917
1 804	0,913	0,913	0,913	0,914	0,914	0,916	0,919
1 843	0,914	0,915	0,915	0,915	0,916	0,918	0,920
1 881	0,916	0,916	0,916	0,917	0,918	0,919	0,922

D.2 Calculations for $R = 200$ mm

Results of the computation of the coupling factor for non-uniform magnetic fields K , as a function of the distance d , are given hereunder in the form of parametric curves, for different values of the radius of the source (parameter r , see Figures D.10 and D.11). Corresponding numerical values are given in Tables D.3 and D.4.

The distance d is the minimum distance between the edge of the disk and the closest part of the source.

D.2.1 Exposure close to the source: $0 < d < 300$ mm



IEC 1584/04

Figure D.10 – Parametric curves of factor K for distances up to 300 mm to a source consisting of a coil and for different coil radius r (homogeneous disk $R = 200$ mm)

Table D.3 – Numerical values of factor K for distances up to 300 mm to a source consisting of a coil (homogeneous disk: $R = 200$ mm)

Distance between the source and the disk mm	Value of the coil radius mm						
	2,5	5	10	20	40	80	160
10	0,018	0,023	0,031	0,043	0,060	0,082	0,102
20	0,044	0,050	0,060	0,076	0,099	0,129	0,163
30	0,071	0,077	0,087	0,105	0,131	0,165	0,205
40	0,097	0,103	0,113	0,131	0,159	0,196	0,239
50	0,122	0,128	0,138	0,156	0,184	0,222	0,268
60	0,146	0,151	0,161	0,179	0,207	0,246	0,293
70	0,169	0,174	0,183	0,201	0,228	0,267	0,315
80	0,190	0,195	0,204	0,221	0,248	0,287	0,336
90	0,211	0,215	0,224	0,240	0,267	0,305	0,354
100	0,230	0,235	0,243	0,259	0,284	0,322	0,371
110	0,249	0,253	0,261	0,276	0,301	0,338	0,386
120	0,266	0,270	0,278	0,293	0,317	0,353	0,401
130	0,283	0,287	0,295	0,308	0,332	0,368	0,415
140	0,299	0,303	0,310	0,323	0,346	0,381	0,427
150	0,315	0,318	0,325	0,338	0,360	0,394	0,440
160	0,329	0,333	0,339	0,352	0,373	0,406	0,451
170	0,343	0,347	0,353	0,365	0,385	0,418	0,462
180	0,357	0,360	0,366	0,377	0,397	0,429	0,472
190	0,370	0,373	0,379	0,390	0,409	0,440	0,482
200	0,382	0,385	0,391	0,401	0,420	0,450	0,491
210	0,394	0,397	0,402	0,412	0,430	0,460	0,500
220	0,405	0,408	0,413	0,423	0,441	0,469	0,509
230	0,416	0,419	0,424	0,434	0,451	0,478	0,517
240	0,427	0,429	0,434	0,444	0,460	0,487	0,525
250	0,437	0,439	0,444	0,453	0,469	0,495	0,533
260	0,447	0,449	0,454	0,462	0,478	0,503	0,540
270	0,456	0,459	0,463	0,471	0,486	0,511	0,547
280	0,465	0,468	0,472	0,480	0,495	0,519	0,554
290	0,474	0,476	0,481	0,488	0,503	0,526	0,561
300	0,483	0,485	0,489	0,497	0,510	0,533	0,567

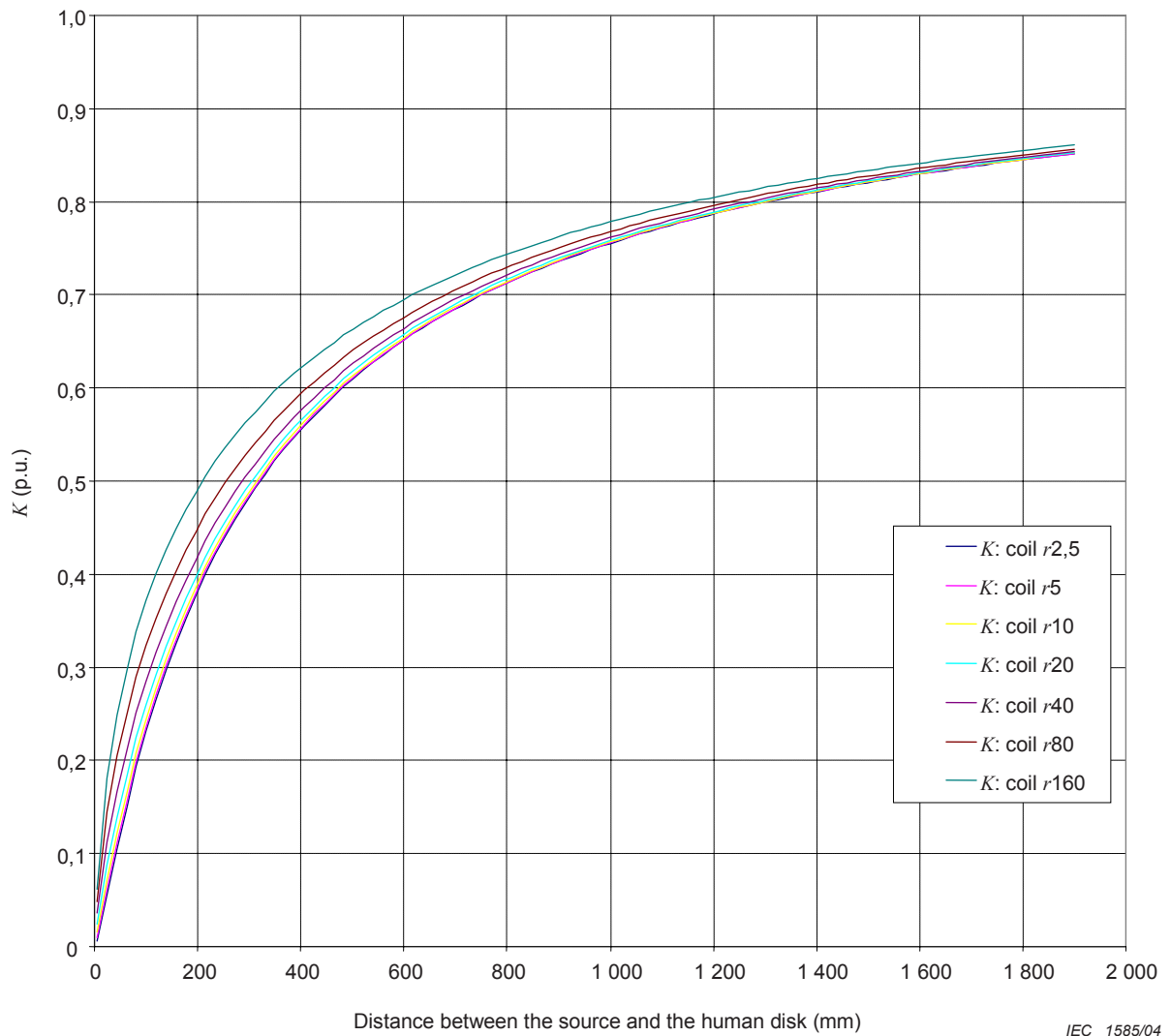
D.2.2 Exposure at higher distance: $0 < d < 1\,900$ mm

Figure D.11 – Parametric curves of factor K for distances up to 1 900 mm to a source consisting of a coil and for different coil radius r (homogeneous disk $R = 200$ mm)

Table D.4 – Numerical values of factor K for distances up to 1 900 mm to a source consisting of a coil (homogeneous disk: $R = 200$ mm)

Distance between the source and the disk mm	Value of the coil radius mm						
	2,5	5	10	20	40	80	160
5	0,006	0,010	0,015	0,024	0,036	0,048	0,062
43	0,105	0,111	0,122	0,139	0,167	0,205	0,249
82	0,193	0,198	0,208	0,224	0,251	0,290	0,339
101	0,232	0,236	0,245	0,260	0,286	0,323	0,372
139	0,298	0,301	0,309	0,322	0,345	0,380	0,426
158	0,327	0,330	0,337	0,349	0,370	0,404	0,449
196	0,378	0,381	0,386	0,397	0,416	0,446	0,488
235	0,421	0,424	0,429	0,438	0,455	0,482	0,521
273	0,459	0,461	0,466	0,474	0,489	0,514	0,550
311	0,492	0,494	0,498	0,505	0,519	0,541	0,574
350	0,521	0,523	0,527	0,533	0,545	0,565	0,596
388	0,547	0,549	0,552	0,558	0,569	0,587	0,616
426	0,570	0,572	0,575	0,580	0,590	0,607	0,633
464	0,591	0,593	0,595	0,600	0,609	0,625	0,649
503	0,610	0,611	0,614	0,618	0,626	0,641	0,664
541	0,628	0,629	0,631	0,635	0,642	0,655	0,677
579	0,643	0,644	0,646	0,650	0,657	0,669	0,689
618	0,658	0,659	0,660	0,664	0,670	0,682	0,700
656	0,671	0,672	0,673	0,677	0,682	0,693	0,711
694	0,683	0,684	0,685	0,688	0,694	0,704	0,720
732	0,695	0,695	0,697	0,699	0,704	0,714	0,729
771	0,705	0,706	0,707	0,710	0,714	0,723	0,738
809	0,715	0,715	0,717	0,719	0,724	0,732	0,746
847	0,724	0,725	0,726	0,728	0,732	0,740	0,753
886	0,733	0,733	0,734	0,736	0,740	0,748	0,760
924	0,741	0,741	0,742	0,744	0,748	0,755	0,767
962	0,748	0,749	0,750	0,752	0,755	0,762	0,773
1 000	0,755	0,756	0,757	0,758	0,762	0,768	0,779
1 039	0,762	0,763	0,763	0,765	0,768	0,774	0,784
1 077	0,768	0,769	0,770	0,771	0,774	0,780	0,789
1 115	0,774	0,775	0,776	0,777	0,780	0,785	0,794
1 153	0,780	0,781	0,781	0,783	0,785	0,790	0,799
1 192	0,786	0,786	0,787	0,788	0,790	0,795	0,804
1 230	0,791	0,791	0,792	0,793	0,795	0,800	0,808
1 268	0,796	0,796	0,796	0,798	0,800	0,804	0,812
1 307	0,800	0,801	0,801	0,802	0,804	0,809	0,816
1 345	0,805	0,805	0,806	0,807	0,809	0,813	0,820
1 383	0,809	0,809	0,810	0,811	0,813	0,817	0,823
1 421	0,813	0,813	0,814	0,815	0,817	0,820	0,827
1 460	0,817	0,817	0,818	0,819	0,820	0,824	0,830
1 498	0,821	0,821	0,821	0,822	0,824	0,827	0,833
1 536	0,824	0,824	0,825	0,826	0,827	0,831	0,837
1 575	0,828	0,828	0,828	0,829	0,831	0,834	0,839
1 613	0,831	0,831	0,831	0,832	0,834	0,837	0,842
1 651	0,834	0,834	0,835	0,835	0,837	0,840	0,845
1 689	0,837	0,837	0,838	0,838	0,840	0,843	0,848
1 728	0,840	0,840	0,840	0,841	0,843	0,845	0,850
1 766	0,843	0,843	0,843	0,844	0,845	0,848	0,853
1 804	0,845	0,846	0,846	0,847	0,848	0,850	0,855
1 843	0,848	0,848	0,849	0,849	0,850	0,853	0,857
1 881	0,851	0,851	0,851	0,852	0,853	0,855	0,860

Annex E (informative)

Simplified approach of electromagnetic phenomena

The magnetic field distribution from the three sources can be calculated using the well-known equations for electromagnetic phenomena. A wire with length dl and supplied by a current I , creates in the air a flux density B and a magnetic field H (Biot and Savart law) as:

$$\vec{B} = \frac{\mu_0}{4\pi} \frac{I d\vec{l} \wedge \vec{r}}{r^3} \quad (\text{E-1})$$

and

$$H = \frac{B}{\mu_0} \quad (\text{E-2})$$

where r is the distance between element dl and the calculation point of B .

This basic relationship shows that B and H are directly proportional to the current, I , in air. Then, the field created by simple sources (such as infinitely long wires, a circular loop, a solenoid,...) can be calculated analytically. Depending on the type of source, B and H decrease rapidly with the distance: $1/r$, $1/r^2$ or $1/r^3$.

More generally, if the Ampere's law is used:

$$\oint_c H dl = nI \quad (\text{E-3})$$

B and H depend on the geometry of the source, the number n of turns (for coils) and the current I flowing in it.

The magnetic flux through a surface S derives from the induction by:

$$\Phi = \iint \vec{B} \cdot d\vec{s} \quad (\text{E-4})$$

In a material, even slightly conducting, an electromotive force (e.m.f.) V is induced by this time varying magnetic flux Φ (Lenz's law):

$$V = - \frac{d\Phi}{dt} \quad (\text{E-5})$$

If the current in the source is sinusoidal, the value of the electromotive force can be expressed in the form:

$$V = \omega \Phi \quad (\text{E-6})$$

where $\omega = 2\pi f$ and f is the frequency.

This electromagnetic field induces eddy current I_i in the material, whose distribution can be characterised by the current density J :

$$I_i = \iint \vec{J} \cdot d\vec{s} \quad (\text{E-7})$$

The intensity I_i of the induced currents in an object placed near the source current, depends directly on this electromagnetic field, and is therefore linked to the geometry of the source, its number of turns, the intensity and the frequency of the current in the inductor, and the distance between the object and the source.

Furthermore, the very rapid increase of magnetic field when approaching the source confirms the importance to study these phenomena and their consequences in the human body placed near to the source.

Annex F (informative)

Analytical calculation of magnetic field created by simple induction systems: 1 wire, 2 parallel wires with balanced currents and 1 circular coil

F.1 Infinite straight wire

Wire characteristics: no section, centred on (0,0,0) and oriented in the z -axis direction.

Magnetic field value (H_x and H_y) at a point (x,y) are given by Ampère's Law

$$\begin{aligned} H_x &= \frac{-I}{2.\pi} \frac{y}{(x^2+y^2)} \\ H_y &= \frac{I}{2.\pi} \frac{x}{(x^2+y^2)} \end{aligned} \quad (\text{F-1})$$

F.2 Two parallel wires with balanced currents

Wires characteristics: no section, centred on (0, $-d/2,0$) and (0, $d/2,0$) and oriented in the z -axis direction.

Distance between the 2 wires = d (in the direction of y axis).

Magnetic field value (H_x and H_y) at a point (x,y):

$$\begin{aligned} H_x &= \frac{-I}{2.\pi} \left[\frac{\frac{d}{2} - y}{(x^2 + (y - \frac{d}{2})^2)} + \frac{\frac{d}{2} + y}{(x^2 + (y + \frac{d}{2})^2)} \right] \\ H_y &= \frac{-I}{2.\pi} \left[\frac{x}{(x^2 + (y - \frac{d}{2})^2)} - \frac{x}{(x^2 + (y + \frac{d}{2})^2)} \right] \end{aligned} \quad (\text{F-2})$$

F.3 Circular coil

Coil characteristics: radius a , located in the XY-plane, centred on point (0,0,0), current I flowing in.

Magnetic field value (radial H_r and vertical H_z) at a point (x,y,z) :

$$H_r = \frac{Ikz}{4\pi r\sqrt{ar}} \left(-K(k) + \frac{a^2 + r^2 + z^2}{(a-r)^2 + z^2} E(k) \right)$$

$$H_z = \frac{Ik}{4\pi\sqrt{ar}} \left(K(k) + \frac{a^2 - r^2 - z^2}{(a-r)^2 + z^2} E(k) \right)$$

with :

$$k = \sqrt{\frac{4ar}{(a+r)^2 + z^2}} \quad (\text{F-3})$$

$$r = \sqrt{x^2 + y^2}$$

$$K(k) = \int_0^{\pi/2} \frac{1}{\sqrt{1 - k^2 \sin^2 \theta}} d\theta$$

$$E(k) = \int_0^{\pi/2} \sqrt{1 - k^2 \sin^2 \theta} d\theta$$

where K and E are elliptical integrals of 1st and 2nd order.

Annex G (informative)

Equation and numerical modelling of electromagnetic phenomena for a typical structure: conductive disk in electromagnetic field

Maxwell's equations are used to describe spatial and temporal electromagnetic phenomena.

In the following equations, displacement currents ($+\frac{\partial \vec{D}}{\partial t}$) are neglected:

$$\text{Curl} \vec{H} = \vec{J} \quad (\text{G-1})$$

$$\text{Curl} \vec{E} = -\frac{\partial \vec{B}}{\partial t} \quad (\text{G-2})$$

$$\text{div} \vec{B} = 0 \quad (\text{G-3})$$

$$\text{div} \vec{J} = 0 \quad (\text{G-4})$$

where [1]³⁾

H is the magnetic field

B is the magnetic induction

E is the electric field

J is the current density

and for materials:

$$\vec{J} = \sigma \vec{E} \quad (\text{G-5})$$

$$\vec{B} = \mu(\vec{H}, \vec{B}) \quad (\text{G-6})$$

where

σ is the electric conductivity

μ is the magnetic permeability

Due to equation (G-4), there is an electric potential T :

$$\vec{J} = \text{Curl} \vec{T} \quad (\text{G-7})$$

In 2D simulation (study in XY -plane), T has only 1 component along z -axis and it can easily be demonstrated [1] that $T \equiv H$.

³⁾ Figures in square brackets refer to the bibliography.

These different equations can be combined to form a single equation:

$$\nabla^2 \vec{H} = \sigma \frac{\partial \vec{B}}{\partial t} \quad (\text{G-8})$$

And in our particular case ("human" object in different fields created by simple source), the magnetic permeability μ equals μ_0 . The equation becomes:

$$\frac{1}{\sigma} \nabla^2 \vec{H} = \mu_0 \frac{\partial \vec{H}}{\partial t} \quad (\text{G-9})$$

The magnetic field can be separated in 2 terms: $H = H_{\text{ex}} + H_r$

H_{ex} : excitation field (created by source currents)

H_r : reaction field (created by induced currents)

The reaction of induced current in the "human" object on the excitation field can be neglected. In this case, the equation (G-9) can be limited to [1]:

$$\frac{1}{\sigma} \nabla^2 \vec{H}_r - \mu_0 \frac{\partial \vec{H}_r}{\partial t} = \mu_0 \frac{\partial \vec{H}_{\text{ex}}}{\partial t} \quad (\text{G-10})$$

For simple excitation coils, the magnetic field H_{ex} can be analytically calculated in air and in body.

Numerical calculation by finite element method in 2D XY -plane allow to solve the equation (G-10). The field $H_r(x,y,t)$, and induced current $J_x(x,y)$, $J_y(x,y)$ are calculated in all points of studied domain ("human" object) by this method:

$$\vec{J} = \text{Curl} \vec{H} = \text{Curl} \vec{H}_r + \text{Curl} \vec{H}_{\text{ex}} \quad (\text{G-11})$$

The term $\text{Curl} \vec{H}_{\text{ex}}$ is null except in the field source, so:

$$\vec{J} = \text{Curl} \vec{H}_r \quad (\text{G-12})$$

in the disk.

Bibliography

- [1] BURAI, N., FOGGIA, A., NICOLAS, A., SABONADIERE, J.C. Electromagnetic field formulation for eddy current calculations in non destructive testing systems. *IEEE Trans. on Magnetics*, November 1982, vol. MAG-18, n° 6.
-

BSI — British Standards Institution

BSI is the independent national body responsible for preparing British Standards. It presents the UK view on standards in Europe and at the international level. It is incorporated by Royal Charter.

Revisions

British Standards are updated by amendment or revision. Users of British Standards should make sure that they possess the latest amendments or editions.

It is the constant aim of BSI to improve the quality of our products and services. We would be grateful if anyone finding an inaccuracy or ambiguity while using this British Standard would inform the Secretary of the technical committee responsible, the identity of which can be found on the inside front cover.
Tel: +44 (0)20 8996 9000. Fax: +44 (0)20 8996 7400.

BSI offers members an individual updating service called PLUS which ensures that subscribers automatically receive the latest editions of standards.

Buying standards

Orders for all BSI, international and foreign standards publications should be addressed to Customer Services. Tel: +44 (0)20 8996 9001.
Fax: +44 (0)20 8996 7001. Email: orders@bsi-global.com. Standards are also available from the BSI website at <http://www.bsi-global.com>.

In response to orders for international standards, it is BSI policy to supply the BSI implementation of those that have been published as British Standards, unless otherwise requested.

Information on standards

BSI provides a wide range of information on national, European and international standards through its Library and its Technical Help to Exporters Service. Various BSI electronic information services are also available which give details on all its products and services. Contact the Information Centre.
Tel: +44 (0)20 8996 7111. Fax: +44 (0)20 8996 7048. Email: info@bsi-global.com.

Subscribing members of BSI are kept up to date with standards developments and receive substantial discounts on the purchase price of standards. For details of these and other benefits contact Membership Administration.
Tel: +44 (0)20 8996 7002. Fax: +44 (0)20 8996 7001.
Email: membership@bsi-global.com.

Information regarding online access to British Standards via British Standards Online can be found at <http://www.bsi-global.com/bsonline>.

Further information about BSI is available on the BSI website at <http://www.bsi-global.com>.

Copyright

Copyright subsists in all BSI publications. BSI also holds the copyright, in the UK, of the publications of the international standardization bodies. Except as permitted under the Copyright, Designs and Patents Act 1988 no extract may be reproduced, stored in a retrieval system or transmitted in any form or by any means – electronic, photocopying, recording or otherwise – without prior written permission from BSI.

This does not preclude the free use, in the course of implementing the standard, of necessary details such as symbols, and size, type or grade designations. If these details are to be used for any other purpose than implementation then the prior written permission of BSI must be obtained.

Details and advice can be obtained from the Copyright & Licensing Manager.
Tel: +44 (0)20 8996 7070. Fax: +44 (0)20 8996 7553.
Email: copyright@bsi-global.com.